

Recent Advances in Polymeric Solvent-Resistant Nanofiltration Membranes

XI QUAN CHENG

State Key Laboratory of Urban Water Resource and Environment (SKLUWRE), School of Chemical Engineering and Technology, Harbin Institute of Technology, Harbin, People's Republic of China

YONG LING ZHANG

State Key Laboratory of Urban Water Resource and Environment (SKLUWRE), School of Chemical Engineering and Technology, Harbin Institute of Technology, Harbin, People's Republic of China

AB InBev Sedrin (Zhangzhou) Brewery Co., Ltd., Zhang Zhou, People's Republic of China

ZHEN XING WANG

State Key Laboratory of Urban Water Resource and Environment (SKLUWRE), School of Chemical Engineering and Technology, Harbin Institute of Technology, Harbin, People's Republic of China

ZHAN HU GUO

Integrated Composites Laboratory, Dan F. Smith Department of Chemical Engineering, Lamar University, Beaumont, Texas 77710

YONG PING BAI, LU SHAO

State Key Laboratory of Urban Water Resource and Environment (SKLUWRE), School of Chemical Engineering and Technology, Harbin Institute of Technology, Harbin, People's Republic of China

Correspondence to: Lu Shao, e-mail: odysseynus@hotmail.com

Received: March 25, 2014

Accepted: June 17, 2014

ABSTRACT: When considering energy consumption and environmental issues, solvent-resistant nanofiltration (SRNF) based on polymeric materials emerges as a process for substituting conventional separation processes of organic solutions, such as distillation, which consume high amounts of energy. Because SRNF does not involve phase transition, this process can potentially decrease the energy consumption and solvent waste and increase the yield of active components. Such improvements could significantly benefit a number of fields, such as pharmaceutical manufacturing and catalysis recovery, among others. Therefore, SRNF has gained a lot of attention since the recent introduction of solvent-stable polymeric materials in the manufacture of nanofiltration membranes. The membrane materials and the membrane structures depending on the fabrication methods determine the separation performance of polymeric SRNF membranes. Therefore, this article gives a comprehensive overview of the current state-of-art technologies of generating membrane materials and corresponding fabrication methods for SRNF membranes made from polymeric materials expected to provide the most benefit. The transport mechanisms and the corresponding models of SRNF membranes in organic media are also reviewed to better understand the mass transfer process. Various SRNF applications, such as in pharmaceutical and catalyst, among others, are also discussed. Finally, the difficulties and future research directions to overcome the challenges faced by SRNF processes are proposed. © 2014 Wiley Periodicals, Inc. *Adv Polym Technol* 2014, 33, 21455; View this article online at wileyonlinelibrary.com. DOI 10.1002/adv.21455

KEY WORDS: Crosslinking, Polyelectrolytes, Polyimides, Solvent-resistant nanofiltration, Transport mechanism

Contract grant sponsor: National Natural Science Foundation of China. Contract grant number: 21177032. Contract grant sponsor: Fundamental Research Funds for the Central Universities. Contract grant number: HIT.BRETIV.201307. Contract grant sponsor: State Key Laboratory of Urban Water Resource and Environment

(Harbin Institute of Technology). Contract grant number: 2014DX05. Contract grant sponsor: Program for New Century Excellent Talents in University. Contract grant number: NCET-11-0805.

Introduction

Energy and environmental issues, including the safe water crisis, global warming, and the shrinking energy supply, have been attracting considerable attention in recent years. Up to now, various technologies have been tentatively explored to obtain clean water, capture “greenhouse” gases, and find alternative energy sources. Membrane separation has emerged as one of the most important technologies by addressing some of the aforementioned pressing problems. Specifically, membrane separation is a low-cost, simple, flexible, and compact process.^{1–8} Although new separation processes are continuously being explored, traditional separation membrane processes are also being used in an increasing number of applications in diverse and advanced fields.

Aqueous nanofiltration (NF) has been an active area of research because of two unique characteristics: a narrow pore size distribution and a high density of surface charges. NF uses a membrane with well-defined pore diameters (0.5–2 nm) and very narrow pore size distribution (molecular weight cutoff: MWCO ≤ 2000 g mol⁻¹) and is a typical pressure-driven separation process without phase transition. NF membranes can be widely used to concentrate, purify, and separate small organic molecules, such as amino acids.⁹ Furthermore, these membranes can be used to remove organic contaminants, such as pesticides.^{10,11} Because of their abundant surface charges that selectively separate ions, NF membranes have also been used to remove heavy metal ions,^{12,13} separate dyes,^{14,15} and soften water.¹⁶ However, in most cases, industrial applications of NF membranes are limited to aqueous solutions. An exciting market can be anticipated based on the development of NF membranes to separate and purify organic media.

NF membranes that separate and purify organic media are named as solvent-resistant nanofiltration (SRNF) membranes or organic solvent nanofiltration (OSN) membranes and have been on the rise since the beginning of this century. In the past, the stability of polymeric NF membranes had hindered their application in organic solvent media. In general, the swelling of polymeric membrane materials significantly reduced the separation efficiency. The worse situation is the occurrence of the dissolution of certain polymeric materials, which results the NF membranes in losing their separation performance totally. Nevertheless, energy efficient and environmentally friendly industrial SRNF processes are urgently needed. For example, SRNF could potentially be valuable in the pharmaceutical manufacturing industry to separate active molecules from solvents. Such a process would decrease energy consumption and solvent waste generation while increasing the yield of active components and could potentially replace conventional distillation methods, which consume large amounts of energy and can potentially inactivate products during the heating process. Since the recent introduction of solvent-stable materials for NF,¹⁷ many studies have focused on the preparation, transport mechanisms, and applications of SRNF.¹⁸ In 2007, Vandezande et al.¹⁸ reviewed several diverse aspects of SRNF, including the preparation and application of SRNF membranes. Since then, polymeric SRNF membranes have experienced significant improvements driven by in-

dustrial need, and a number of significant fundamental studies based on systematical investigations covering membrane materials, membrane fabrication technology, and membrane separation mechanisms have been reported by various groups. Take some examples, Soroko et al.^{19–21} have published several studies of the effect of membrane formation parameters on the performance of polyimide (PI) SRNF membranes. They illustrated that the rejection of membranes can be predicted by the total solubility parameter ($\Delta\delta_t$) of the phase inversion system if the values of $\Delta\delta_t$ are close.¹⁹ Moreover, they report that the molecular weight of PI should be maintained between 35,000 to 80,000 g mol⁻¹ for optimal performance.²¹ Based on the aforementioned results, the fabrication of PI SRNF membranes can be improved by replacing toxic solvents with environmentally friendly dimethylsulfoxide (DMSO)/acetone solvents during phase inversion by adjusting the total solubility parameter.²² Darvishmanesh et al.^{23–25} have developed a transport mechanism based on systematical works. Initially, the mutual affinities of membranes and solvent were found to affect the permeability of the solvent in dense membranes; however, the viscosity of solvents should primarily determine the permeability of porous membranes.²³ They then developed a convective-diffusive transport model (details can be found in the section The Solvent Transfer Models), which can accurately estimate the pure solvent flux of different solvents through three commercial SRNF membranes.²⁴ Furthermore, a new model, the coupled series-parallel for transport of solvents through SRNF membranes, has been proposed.²⁵ This model is suggested to accurately predict the transport flux of different solvents through two types of ceramic membranes with the deviations less than 4.2%. However, this new model may show higher deviations when predicting solvent permeability in certain circumstances (e.g., when the swelling effect of polymeric membranes is considered).

Therefore, this timely review will elucidate recent developments in polymeric SRNF membrane technologies based on state-of-the-art works since 2007. In this review, the fabrication and materials of SRNF membranes are introduced in the second section. The transport mechanisms that can accurately predict the rejection and solvent permeability are systematically explained in the third section. The diverse and advanced applications of SRNF membranes are comprehensively discussed in the fourth section. Finally, the future research outlook and promising prospects for SRNF membranes are presented, which will inspire and stimulate readers to make potential contributions in this developing field.

Fabrication and Polymeric Materials of SRNF Membranes

Membrane materials significantly influence the separation performance of all membrane separation processes, including the SRNF membrane separation process. Generally, the materials used to fabricate SRNF membranes can be classified into three types: (a) organic polymers; (b) inorganic materials (oxides, ceramics, metals); and (c) organic-inorganic hybrids. Because of the dominating use and rapid development of organic polymer

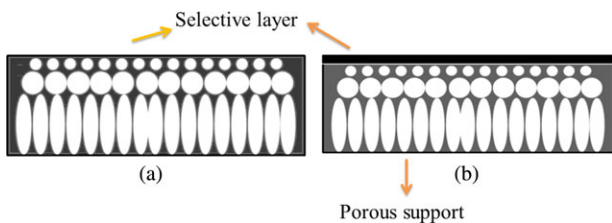


FIGURE 1. Schematic representation of major polymeric membrane types used for SRNF: (a) asymmetric membrane, (b) composite membrane.

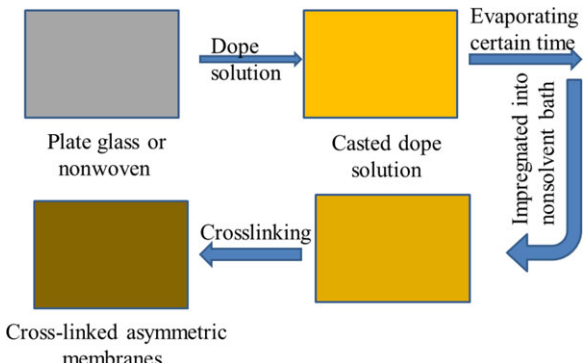


FIGURE 2. Schematic representation of polymeric SRNF membranes fabricated by phase inversion.

materials, this section will mainly focus on polymer materials for the fabrication of SRNF membranes, although inorganic and organic–inorganic hybrid materials have complementary advantages.

On the other hand, various membrane fabrication techniques can be adopted to gain different cross-sectional structures with diverse performances depending on the membrane material (asymmetric or composite membranes, as shown in Fig. 1). The phase inversion technique is typically used to fabricate asymmetric membranes,²⁶ whereas composite membranes are fabricated in two steps: (a) the fabrication of support membrane and (b) the fabrication of ultra-thin selective layers. Nonsolvent-induced phase separation (NIPS) and thermally induced phase separation are two basic approaches to obtain various types of supports. A number of diverse strategies are used to prepare thin-selective layers, such as the interfacial polymerization (IP) technique,^{27–32} coating-crosslinking,^{19–22} and layer-by-layer (LBL) self-assembly.^{33–37} A comprehensive summary of the materials and fabrication methods of polymeric SRNF membranes is listed in Table I.

THE FABRICATION OF POLYMERIC SRNF MEMBRANES

The majority of polymeric SRNF membranes are fabricated by NIPS. A schematic diagram of the phase inversion process is illustrated in Fig. 2.^{38–41} The cross-sectional areas of membranes fabricated by this method are structurally asymmetric. First, the selected polymer is dissolved in a liquid mixture containing primary solvent, cosolvent, and the necessary additives to generate a homogenous doping solution. Second, the doping solution is

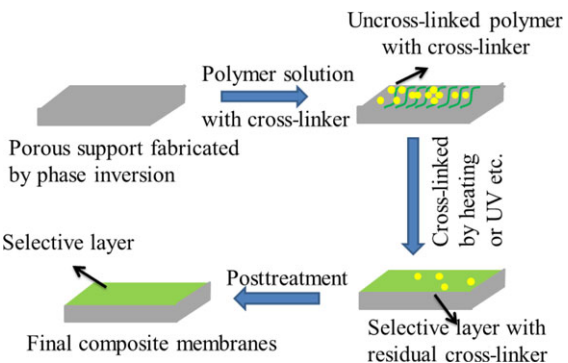


FIGURE 3. Schematic representation of polymeric SRNF membranes fabricated by dip-coating process.

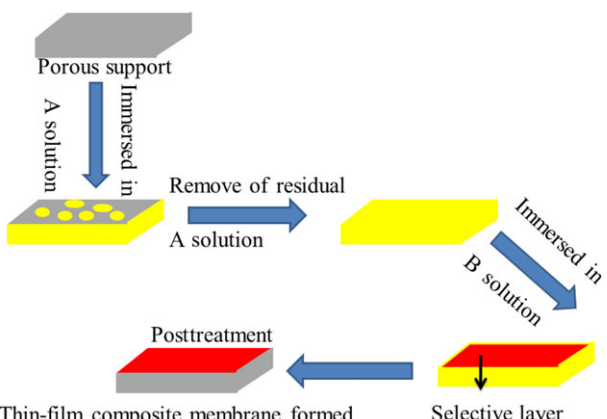


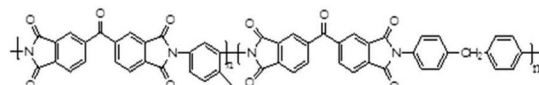
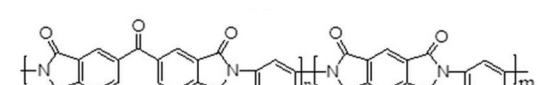
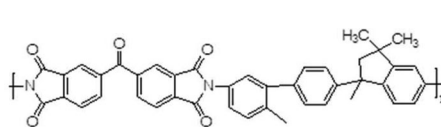
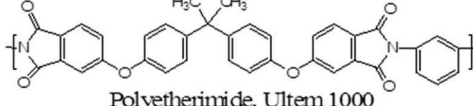
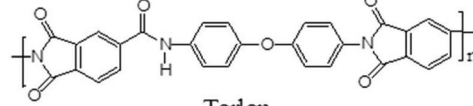
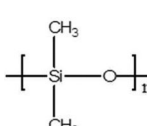
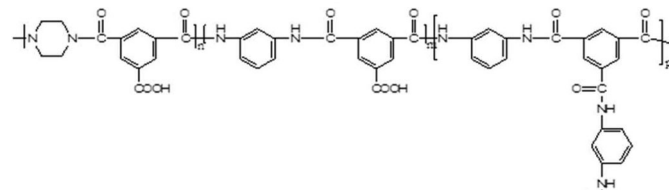
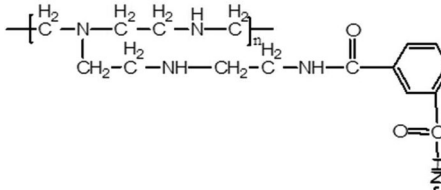
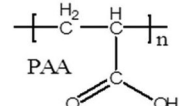
FIGURE 4. Schematic representation of interfacial polymerization process.

degassed and cast onto a flat glass surface or nonwoven fabric to form flat membranes. After evaporating the solvent for a few seconds, the cast membranes are immersed in a nonsolvent (typically water) bath to induce the phase inversion (separation). The obtained asymmetric membranes are immersed in the water bath several times to ensure that any extraneous substances (solvent, cosolvent, and additives) are completely removed. If desired, the membrane can then be post-treated prior to use or storage.

The preparation of the selective layer is crucial in the fabrication of SRNF. In essence, the selective layer of SRNF membranes can be prepared by three approaches. First, coating followed by cross-linking (as Fig. 3 shown) is a simple and straightforward method. The solute in the coating solution can be the cross-linkable polymer or active monomers that can polymerize under certain circumstances to form selective layers on the supports. Second, IP is based on a polymerization reaction that takes place at the interface between two immiscible phases (Fig. 4), such as an aqueous phase and a hexane phase. In fact, IP is a practical process to prepare NF and reverse osmosis (RO) membranes^{42,43} in industry; commercial NF membranes have been successfully manufactured using this process. Polyether-sulfone (PES) or polysulfone (PSF) supports are typically used in commercial composite membranes. However, such support materials swell significantly in polar solvents, which limit broader

TABLE I

Polymers Used to Prepare the Selective Layers of Solvent-Resistant Nanofiltration Membranes

Membrane Materials	Structure	Cross-Section	References
PI		Asymmetric	19–22,46,47,52,59,63
		Asymmetric	19
		Asymmetric	19,46,55,57,58,60
		Asymmetric	19,46
		Asymmetric	46
PDMS		Composite (PAN as Support)	67–76
PA		Composite (PAN as Support)	27,30,31
		Composite (PES or PP as Support)	28,29,80
PEs		Composite (PAN as Support)	33

Continued

TABLE I
Continued

Membrane Materials	Structure	Cross-Section	References
		Composite (PAN as Support)	33–37
		Composite (PAN as Support)	34,36,37
		Composite (PAN as Support)	35
		Composite (PAN as Support)	35
PTMSP		Composite (PAN or cellophane as Support)	98–101
PIM		Composite (PAN as Support)	102
PPy		Composite (PAN, PI and PSF as Support)	104,203
PU		Composite (PAN as Support)	105
PPSU		Asymmetric	108,109
PANI		Asymmetric	110–113
PBI		Asymmetric	115,116

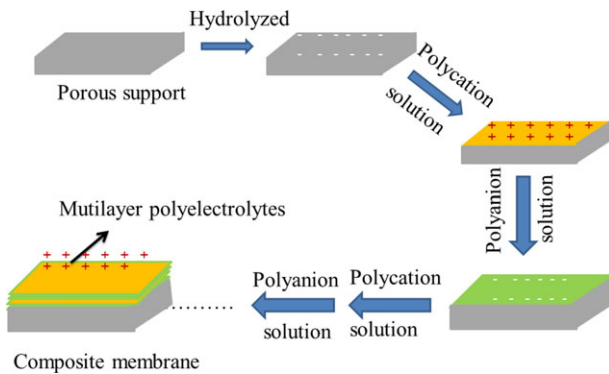


FIGURE 5. Schematic representation of polymeric SRNF membranes based on PAN substrates fabricated by layer-by-layer self-assembly process.

applications of SRNF. Significant efforts should be made to solve this problem and find suitable support materials, which will be discussed in the section PA for SRNF Membranes. Third, LBL self-assembly is a technique in which different molecules assemble into an ordered structure via intermolecular forces, such as hydrogen bonds and electrostatic attraction of polyelectrolytes (PEs) (Fig. 5). This technique has mostly been used in the manufacture of separation membranes such as NF, RO, and forward osmosis.^{33,37,44,45} As mentioned above, the SRNF fabrication process strongly depends on the materials used. Therefore, the following section will discuss the polymeric materials used for SRNF membranes.

THE POLYMERIC MATERIALS FOR SRNF MEMBRANES

The type of polymeric material significantly influences the separation performance of SRNF membranes. As mentioned above, membrane materials had limited the developing of the application of NF technique in organic circumstances. To be used in the fabrication of SRNF, a support should be stable in the solvent and compatible with the selective layer material to avoid peeling under swelling conditions. Polyacrylonitrile (PAN), polypropylene (PP), and PI are most often used because they are mechanically stable, can be further cross-linked, and can be applied in thin and defect-free layers. Because selective layer determines the membrane performance, this section mainly discusses the selective layer materials, unless the support plays a vital role in determining the performance of polymeric SRNF membranes. For composite membranes, the selective layer of SRNFs may be made of different materials from support membranes to optimize performance. Various materials can constitute the selective layer, including PI, polydimethylsiloxane (PDMS), polyamide (PA), and PEs, among others. In fact, these materials have been used to fabricate NF membranes in aqueous solutions for a long time. And in recent years, great efforts have been made to find ways to broaden these commonly screened materials for the fabrication of advanced SRNF membranes. When applied in the fabrication of aqueous NF membranes, these polymeric materials typically did not need the cross-linking protocol. However, for the SRNF applications, the higher interaction between solvents and polymeric materi-

als makes used materials dissolving or swelling in some specific solvents, such as *N,N'*-dimethyl formamide (DMF), *N,N'*-dimethyl acetamide (DMAc), and so on. To broaden the applications of these materials in the fabrication of advanced SRNF membranes, enhancing the interactions among macromolecules in polymeric materials is essential. For PI, cross-linking is a well-documented method to solve the problem since PI has unique reactive groups.^{46–52} For PDMS as a kind of dense and easily swelling materials, the blending approach by the addition of rigid fillers (montmorillonite, mica, zinc oxide, zeolite A, 15 ZSM-5, zeolite Y, silicalite, and so on) seems the effective way. For PA with the well cross-linked structure, the affinity between PA and the used solvents and the stability of the support should be further improved.^{28–31} For PEs as usually water-soluble polymers, introducing crosslinkable chemical groups or enhancing the intertwined and electrostatic attraction among PEs is feasible ways.^{33–37}

PI for SRNF Membranes

Because PI is stable in a wide range of solvents, readily forms films and cross-links easily in the solid state,^{46–52} it is suitable to fabricate SRNF membranes. Two steps are generally needed to make SRNF membranes from PI, including phase inversion and cross-linking by thermal treatment,⁵³ UV irradiation,⁵⁴ or chemical reactions.^{19–21,46,55,56} P84 and Matrimid[®] are two types of commercial PI products that have been widely used to fabricate SRNF membranes.^{19–22,46,47,52,55,57–60} The PI should be dissolved in polar solvents such as DMAc, *N*-methyl-2-pyrrolidone (NMP), and DMSO to form a homogeneous doping solution and optimize performance. The doping solution is then degassed before casting on a nonwoven support. After total phase inversion in aqueous solutions, the membrane is immersed in a cross-linker/isopropanol (IPA)^{19–21} or methanol^{46,48,55} solution to swell the polymer chains and ensure adequate contact between the cross-linkers and the polymer chains to facilitate the cross-linking reaction. (Phase diagrams are helpful for better understanding of the relationships between membranes structure and the composition of the doping solutions. The corresponding information was introduced in Refs. 18 and 20 in detail.) The detailed cross-linking mechanism is shown in Fig. 6. The commonly screened cross-linkers are diamines, such as ethylenediamine, hexanediamine, *p*-xylylenediamine (XDA), diethylenetriamine, *N,N'*-dimethylethylenediamine, and so on.^{19–22,44,55,60} After cross-linking, PI membranes are usually immersed in an oily solution to avoid pore collapse. This solution typically consists of 40 vol% toluene, 40 vol% 2-methyl-4-pentanone, and 20 vol% mineral oil.^{57,58} Finally, PI SRNF membranes should be thermally treated for approximately 1 h in a vacuum oven at 65°C to enhance the separation performance.^{55,57,58,60}

Soroko et al.^{19–21} have published numerous valuable studies on membrane formation parameters, such as the composition of the doping solution, the evaporation step, and the physical and chemical properties of PI materials. The composition of the doping solution affects the separation properties of SRNF membranes. These parameters include the type of polymer materials, the polymer concentration in the doping solution and the type and content of solvents and cosolvents.^{19–21} With the exception of the polymer concentration in the doping solution, the

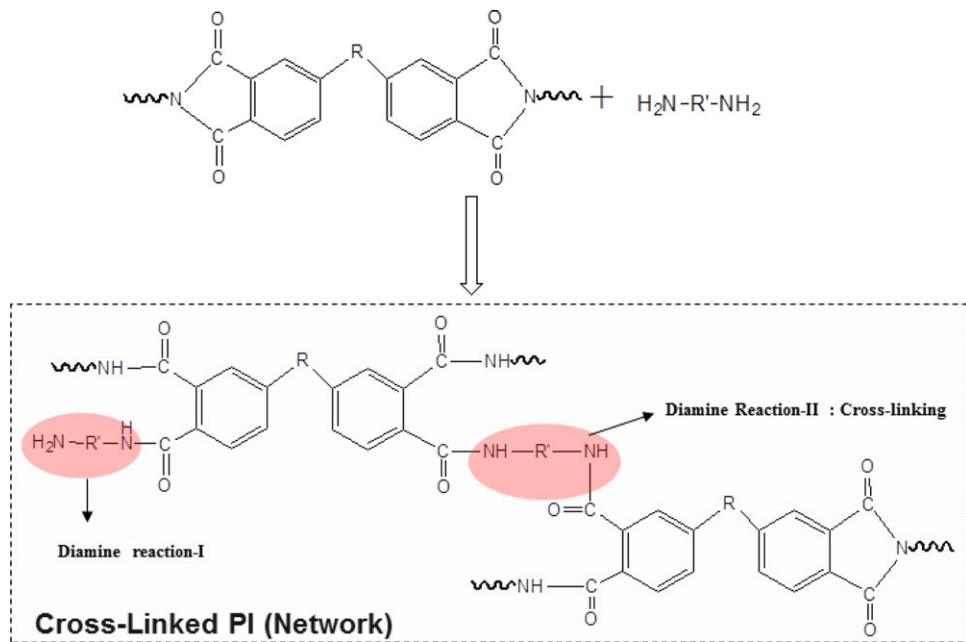


FIGURE 6. Reaction mechanism of cross-linked polyimides by diamines.⁴⁹

total solubility parameter, which is a function of other important factors, primarily influences the properties of SRNF membranes. The total solubility parameter ($\Delta\delta_t$) can be calculated from the solubility parameters between solvent and polymer ($\Delta\delta_{S/P}$), nonsolvent and polymer ($\Delta\delta_{NS/P}$), and solvent and nonsolvent ($\Delta\delta_{S/NS}$) ($\Delta\delta_{S/NS}$ represents the interaction between solvents and nonsolvents, which reflects the diffusion rate of solvent in water). A higher total solubility parameter of the doping solution results in a tighter membrane with increased rejection which can be used to predict the rejection of the membrane as a function of the polymer/solvent/nonsolvent systems.^{19–21} Specifically, SRNF membranes with higher cosolvent contents reject more styrene oligomer than those with lower cosolvent contents. Furthermore, the presence of cosolvents in a certain polymer/solvent solutions decreases the thickness of the membranes. They attributed this to the changes of the diffusion rate ratio of solvent and water. The higher the diffusion ratio is, the denser selective layer and the lower final thickness formed. The cosolvents generally have a low affinity for water (the higher value of $\Delta\delta_{S/NS}$), which decreases the driving force for water diffusions.²⁰ They fabricated PI membranes in DMF and in DMF/1,4-dioxane (as a cosolvent). They found that the thickness of the membranes fabricated in DMF was about 114.7 μm . However, when the mass ratio of the DMF/tetrahydrofuran (THF) is 3/1, 1/1, and 1/3, the thickness of the PI membranes decreased to 110.5, 97.1, and 83.5 μm , respectively. Therefore, the existence of cosolvent increases the rejection of SRNF membranes. The evaporation step and chemical properties of the polymer materials also significantly affect the performance of SRNF membranes.^{20,21} Traditionally, evaporation prior to immersion in a water bath is considered a necessary step to fabricate SRNF membranes.^{18,52,57,61} Soroko's²⁰ pioneering work indicated that longer evaporation times to completely evaporate the solvent can reduce the flux without improving the rejection

of SRNF membranes. Similar results have also been observed in other studies.^{62,63} The effects of the molecular weight and chemical structure of PI on the performance of SRNF membranes have been investigated by Soroko et al.²¹ To obtain a defect-free membrane and maintain the polymer solution at an appropriate viscosity, the molecular weight of PI should be maintained between 35,000 and 80,000 g mol⁻¹. In addition, the random configuration membranes fabricated from PI have a higher flux and lower rejection compared with membranes fabricated from commercial P84 (block PI polymer). Vandezande et al.⁵⁷ also studied the effects of phase inversion parameters. In a large study of SRNF membranes fabricated using various preparation parameters during the phase inversion process, they found that the PI concentration, addition of nonsolvent, and the addition of cosolvent primarily contributed to the high performance SRNF membranes.

As mentioned above, the cross-linking process (reaction) significantly affects the performance of PISRNF membranes. Therefore, the reactivity of PIs and diamines (cross-linkers), cross-linking time, hydrophobicity of diamines, steric configuration of diamines and PIs, and the inter-chain space of the solid membranes critically influence the performance of SRNF membranes. Vanherck et al.⁵⁵ investigated the effects of cross-linking time on the properties of SRNF membranes using XDA as the cross-linker. During the first 5 min of the reaction, the flux decreased dramatically with the cross-linking time. After this point, the flux only slightly changed as the cross-linking time increased. However, the rejection showed an opposite trends. In addition, the cross-linked SRNF membranes were stable in aprotic solvents (DMF, NMP, DMAc, and DMSO). In DMF, the cross-linked SRNF membranes showed a permeability of 5.4 L m⁻² h⁻¹ bar⁻¹ with high rejections of rose bengal (RB) (>98%) and methyl orange (MO) (>95%). Vanherck et al.⁴⁶ also studied the effects of cross-linkers on the performance of PI SRNF membranes in which

water coagulation was utilized. Because the cross-linking reaction can proceed in aqueous media without the emission of organic solvents (such as methanol and IPA),⁴⁶ this approach was considered economically and environmentally advantageous. Almost simultaneously, Soroko et al.²² also published a study on the environmentally friendly fabrication of SRNF membranes. In this work, toxic solvents such as DMF/1,4-dioxane were replaced with an environmentally friendly DMSO/acetone system. To further diminish the environmental impact, IPA was successfully replaced with water in the cross-linking step. They stated that the MWCO of fabricated membranes by this new method was lower than that of conventional membranes. The typical membranes shows excellent comprehensive performance with DMF flux of $137 \text{ L m}^{-2} \text{ h}^{-1}$ under the operating pressure of 30 bar and the MWCO of 350 g mol^{-1} . This method is promising because it is environmentally friendly.²²

PDMS for SRNF Membranes

PDMS is a type of organosiloxane elastomeric polymer normally classified as a "silicone." PDMS consists of a siloxane (Si–O) backbone substituted with methyl groups that give it a high free volume fraction. Therefore, PDMS is usually applied in pervaporation and gas separations because it provides high diffusion coefficients for solvents and gases.^{64–66} In fact, cross-linked PDMS is chemically stable in mostly organic solvents. To fabricate a high-performance selective layer, porous supports are usually impregnated with water to prevent extensive intrusion.¹⁸ After solvent evaporation, cross-linking can be completed at elevated temperatures^{67–71} or by irradiation.^{71,72} However, the swelling of PDMS in some apolar solvents can reduce the selective performance and possibly induce the peeling of the selective layer from the support. These are the main problems that limit the applications of PDMS. Therefore, the factors that affect the swelling of PDMS must be clarified. Recently, some researchers have attempted to elucidate some of these aspects even though the swelling process is rather complicated.^{67,72–77} The swelling of PDMS is primarily determined by the interactions between the solvent and PDMS. The polarity of the solvent, the affinity between PDMS and the solvent, and the cross-linking density of PDMS are the most important factors influencing the swelling process.⁶⁷ For PDMS/PAN composite membranes, the swelling occurs in low polarity solvents, such as n-hexane and xylene. However, in some high polarity solvents (such as alcohols), the composite membrane shrinks. After significant swelling, the viscosity of solutions is the predominant factor that determines the permeability of the solvent.⁶⁷ In addition, the applied pressure influences the swelling of PDMS. According to a report by Tarleton et al.,⁷² the thickness of PDMS increased by 170% after swelling without applied pressure; however, this increase was only 20% when 20 bar of pressure were applied because the pressure compacts the polymer. Many other studies have attempted to minimize the swelling of PDMS.^{69–71,78} Specifically, zeolite can be used as a kind of filler for PDMS to limit its swelling by increasing the solvent permeability.^{69–71} They found that effect of zeolite on the limitation of swelling of PDMS is due to incorporating a silicalite zeolite in PDMS.^{69–71} By doping with USY or ZSM-5, the zeolite filled PDMS membranes show less swelling

(over 50% swelling degree decreased) performance with higher rejections and more stability for nonpolar solvents at 50°C.

In addition, the literature details a new type of composite capillary membrane.⁶⁸ Capillary membranes can provide a high surface to volume ratio and do not require spacers, which enables the design of more compact and simpler modules. Dutczak et al.⁶⁸ fabricated composite capillary membranes with PDMS on α -alumina capillary supports. They found that pre-cross-linking the PDMS coating solution was necessary to fabricate a thin selective layer without defects. The composite membranes were stable in toluene over 40 h with a permeability of $1.6 \text{ L m}^{-2} \text{ h}^{-1} \text{ bar}^{-1}$ and a MWCO of 500 g mol^{-1} .⁶⁸

PA for SRNF Membranes

PA can be used as the selective layer for SRNF membranes using IP technology. The solvent-resistant performance of PA composite membrane is mainly determined by the support because the cross-linking density of the PA selective layer is rather high. Therefore, choosing a suitable support material is important to maximize the performance of the SRNF. PES or PSF are the most commonly used support materials for commercial composite membranes. These materials swell heavily in polar solvents. Therefore, PAN containing carboxylic acid groups at its surface were investigated as a potential support material because solvent resistance can be improved by the induced ionic bonds between the PA top-layer and the PAN support.⁷⁹ Kim et al.²⁷ investigated the performance of PA/PAN composite SRNF membranes with different solvents. Methanol and acetone had the highest permeability, followed by ethanol and IPA. The rejection of oleic acid in ethanol exceeded 90%. Interestingly, hexane could not pass through such membranes because it showed the lowest dielectric constant (nonpolar) and hydrophobicity. Sirkar and co-workers^{28,29,80} carried out a series of works focusing on the synthesis of highly solvent-resistant PA composite SRNF membranes on PP supports by the IP of polyetherimide (PEI) and isophthaloyl dichloride. The rejection of brilliant blue R could be adjusted to 88% in methanol with a permeability of $1.2 \text{ L m}^{-2} \text{ h}^{-2} \text{ bar}^{-1}$ ($3.4 \times 10^{-7} \text{ cm}^3 \text{ cm}^{-2} \text{ s}^{-1} \text{ kPa}^{-1}$). After 10 weeks of continuous measurement, the composite SRNF membrane was highly stable in alcohols and aromatic hydrocarbons. Furthermore, multiwalled carbon nanotubes (CNTs) were incorporated into the PA selective layer during the IP process. The methanol permeability of the CNTs/PA/PP composite SRNF membrane was almost an order of magnitude higher than that of the PA/PP composite SRNF membrane without CNTs. Moreover, PES was also used as a support to fabricate CNTs/PA/PES composite SRNF membranes. CNTs/PA/PES composite SRNF membranes showed outstanding stability against methanol and a 91% rejection of brilliant blue R. However, the reason underlying this enhanced solvent permeability is not clear and requires further investigation.²⁹

Solomon et al.^{30,31} have also published interesting works on the fabrication of SRNF membranes by IP. They found that the nonpolar solvent flux of composites membranes polymerized from m-phenylenediamine (MPD) and trimesoyl chloride (TMC) increased after treatment with an active solvent (DMF or DMSO). Moreover, the membranes were further hydrophobically

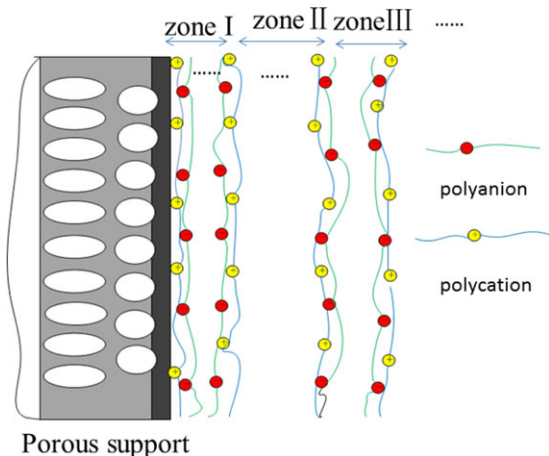


FIGURE 7. Schematic representation of three zones in polyelectrolytes SRNF membranes.

modified to enhance the nonpolar solvent permeability. Pentafluoroctanoyl chloride or 2,2,3,3,3-pentafluoropropylamine were introduced into the polymer network of selective layers polymerized from MPD and TMC. In response, the toluene permeability of the novel composite membranes dramatically increased from 0.31 to $3.8 \text{ L m}^{-2} \text{ h}^{-1} \text{ bar}^{-1}$.^{30,31}

PEs for SRNF Membranes

The LBL self-assembly of PEs on porous supports is a simple, versatile, and environmentally benign technique to fabricate the active layer. SRNF membranes fabricated by the LBL deposition of PEs have two obvious advantages: (a) the thickness of the active layer is adjustable; and (b) the types of charges on the surface of PEs composite SRNF membranes are adjustable. The adjustable thickness of selective layers increases the permeability of PEs composite SRNF membranes by optimizing the number of deposited PEs layers and preparation conditions (such as pH, the concentration of inorganic salts, etc.). The rejection of different salts or charged dyes by these membranes can also be manipulated by modifying the types of charges on their surface.³³ In addition, the structure of PEs membranes can be explained by the model proposed by Ladam et al.⁸¹ Three zones exist in the cross-section of PEs composite SRNF membranes, which are depicted in Fig. 7. Zone I consists of a few layers closed to the support membrane, which is mainly affected by the support, and Zone III consists of a few layers near the edge of the upper surface of the membrane, which is influenced by the interface between the air and the top surface of the membranes. Zone II is the bulky region between zone I and zone III, which is not affected by the interface or support. The intrinsic charge compensation is the main way in which PEs charge compensates in this zone. Initially, zone I and zone III are formed when the first layer of PEs are deposited. As the number of the deposited layer increases, zone II emerges and any additional multilayer growth occurs only in zone II.

A few studies have examined PEs composite SRNF membranes to date.^{34,82–91} Li and co-workers^{33–37} studied a series of SRNF membranes fabricated by the self-assembly LBL method. They fabricated PEs composite SRNF membranes by combining

polydiallyldimethylammonium chloride polycations with various polyanions, including polyacrylic acid (PAA)³³, sulfonated poly(ether ether ketone)^{34–36}, poly(sodium styrene sulfonate), and poly(vinyl sulfate).³⁷ Their results illustrated that the thickness of PEs composite SRNF membranes affect the permeability of solvents^{33–37} and can be adjusted by the number of deposited layers as well as the conformation of the PEs chains. Furthermore, the conformation of PEs chains strongly depends on the density of electrostatic charges, the pH value, and the ionic strength of solutions. The rejection of different dyes by PEs membranes significantly depends on the type of charges on the top layer of the membranes, the type and quantity of the dye electric charges, and the number of deposited layers.

Because the active layer of PEs composite membranes is denser and their mass transfer resistance is higher, the permeability of membranes decreases as the number of deposited layers increases. Furthermore, the density of electrostatic charges affects the permeability of membranes by adjusting the stretch (conformation) of PEs chains. PEs chains with a higher density of electrostatic charges tend to better match the distances between charged groups in the polycation and the polyanion, leading to a flatter deposition with less loops, which accounts for higher retentions and higher permeability of membranes with a higher density of electrostatic charges.^{35,92} The effects of pH and ionic strength on the thickness and permeability of the membranes is a function of the type of polyion used. The thickness of membranes fabricated with the LBL technique using polydiallyldimethylammonium chloride and PAA decreases as the pH value of the deposition solution increases from 2 to 4. This phenomenon can be attributed to a decrease in the segmental population of deposited loops per coating when the charge of the PAA chains increases (ionized). Nevertheless, a significant increase in thickness was observed when the pH value of the solution was further increased beyond 4. A similar phenomenon has been observed by Shiratori et al.⁹³ and Park et al.⁹⁴ Furthermore, the ionic strength, which is determined by the salt concentration in the deposition solution, affects the thickness and permeability of membranes by tuning the conformation of PEs chains. When the salt concentration is increased, the electric potential around the polymer chains decays faster because the PEs adsorbs in more "loopy" conformations. Therefore, the thickness of the membranes increased almost linearly with the salt concentration.^{33,37,95} However, an increase in the salt concentration can also lead to the decomposition of multilayers, which might eventually decrease the thickness.^{33,96,97} The permeability showed a similar trend because adding salt to the PEs solutions leads to the deposition of more loopy-structured chains, which consequently makes the material less dense. The rejection performance strongly depends on the type of charges on the top layer of the PEs composite membranes. Positively charged membranes on the top surface show a higher rejection of positively charged dyes due to static repulsion and vice versa.³⁷ Moreover, the membranes show a higher rejection of the same charged dyes with a high valence state than of mono-charged dyes due to the Donnan effect. (The Donnan effect is a common phenomenon in physical chemistry. For example, when electrolytes solutions pass through a positive membrane, positive charged ions have more resistance for electrostatic repulsion between the ions and the membranes. The higher valences the ions charge, the more resistance of the ions own. Therefore, the rejection of ions is in

the following order: $M^{3+} > M^{2+} > M^{+1}$. Although in solvent, this effects are much lower, for PEs membranes, the effects could not be neglect as reported.^{33–37} Interestingly, the rejection was independent of the number of bilayers in the membrane once zone I and zone III were formed.³⁷ As a result, adjusting the number of the deposited bilayers can increase the permeability of the membrane. The solvent-resistant performance showed that the membranes were stable in solvents such as DMF, IPA, and THF.^{33–37} These PEs membranes have a high potential for purifying or recovering charged solutes, such as dyes, amino acid, and certain charged catalysts. These membranes show rejections above 97% of PB and permeabilities around $0.03\text{--}0.2 \text{ L m}^{-2} \text{ h}^{-2} \text{ bar}^{-1}$ in IPA.

Other Polymer Materials for SRNF Membranes

In recent years, many researchers have attempted to develop new materials to fabricate SRNF membranes. Among these developed materials, glassy polymers with a high free volume fraction have generated significant concern due to their intrinsic microporosity.^{98–103} NF membranes based on these polymers are expected to have a high flux and result in a high rejection due to their higher diffusion. Volkov et al.^{98–101} fabricated SRNF membranes using a type of glassy polymer with a high free volume fraction (up to 25%), named poly(1-(trimethylsilyl)-1-propyne) (PTMSP). Specifically, they coated a cellophane support with a layer of PTMSP to prepare a composite SRNF membrane. With respect to the chemical structure (stability), PTMSP is inherently stable in alcohols, ketones, and certain aliphatic hydrocarbons. They found that dense PTMSP membranes with a thickness of approximately 24–30 μm were much more permeable to ethanol than commercial silicone-based membranes.⁹⁸ Furthermore, PTMSP has also been used to fabricate thin selective layers on a porous PAN support. Optimized PTMSP/PAN composite membranes with a selective-layer thickness of approximately 1 μm showed an ethanol permeability of $3.8 \text{ kg m}^{-2} \text{ h}^{-1} \text{ bar}^{-1}$ and a 90% rejection of Remazol Brilliant Blue R (MW 626.5) at 5 bar. Moreover, they also found that the viscosity of the solution, rather than the swelling of composite membranes, is the dominant factor affecting the permeability of the composite membrane.¹⁰⁰

Polymers with intrinsic porous and derived copolymers attract a lot concern recently for their high free volume and ultra-stable in polar (alcohols, ketones), aromatic (benzene, toluene), nonpolar (alkanes), or aprotic polar (DMF, NMP, DMSO) solvents.^{102,103} Fritsch et al.¹⁰² designed several kinds of polymers of intrinsic microporosity (PIMs) and found that the PIMs can also be generated by coating the material on porous PAN membranes, followed cross-linking with PEI to fabricate a new type of composite SRNF membrane. In a continuous experiment that was recorded over 200 h, the permeability of the composite membrane was extremely stable, and the 90% rejection of the composite membrane was less than 200 g mol^{-1} at 30 bar.¹⁰²

Polypyrrole (PPy),¹⁰⁴ polyurethanes (PU),¹⁰⁵ chloromethylated/quaternized poly(phthalazinone ether sulfone ketone),¹⁰⁶ phenolphthalein-based poly(ether ether ketone),¹⁰⁷ polyphenylsulfone (PPSU),^{108,109} polyaniline (PANI),^{110–113} segment polymer networks,¹¹⁴ polybenzimidazole (PBI),^{115,116} polyether etherketone,^{117,118} PSF,^{119–121} and organic–inorganic hybrid materials^{122,123} have been applied to synthesize the selective lay-

ers on a porous support. Of the various materials that have recently been developed for SRNF applications, PANI-based composite membranes deserve significant attention because PANI composite membranes been successfully synthesized at the laboratory scale^{110,112,113} and spiral-wound PANI composite membranes could be used for industrial-scale separations.¹¹¹ These spiral-wound modules were stable in acetone, THF and DMF and can be easily used even after the membranes have been dried out. The MWCO of such membranes was 300 g mol^{-1} in DMF and showed a high potential for SRNF and solvent exchange applications. The work reported by Li et al.¹¹⁴ focused on the fabrication of SRNF membranes with segmented polymer networks. These segmented polymer networks consist of two-component networks of covalently interconnected hydrophilic/hydrophobic phases with a cocontinuous morphology and covalent bonds between the two phases in the segmented polymer networks. These bonds limit the maximal degree of swelling and prevent the swollen network structure from disintegrating. This process accounts for the highly solvent-resistant performance of these membranes. All of the developed SRNF membranes showed a high permeability to DMF and a low permeability to IPA because of the swelling properties of the segmented polymer networks. These swelling properties are controlled by the fraction of hydrophilic segments in the segmented polymer networks. However, the retention of RB by all membranes was higher than 99% in IPA and DMF.¹¹⁴

Summarily, the development of advanced SRNF membranes mainly focuses on finding ways to modify general (aqueous) NF materials. Because great efforts have been made on this direction in recent years, only few works have been carried out for exploring new materials through certain chemical reactions to require unique performance.^{102,106,107,114,124} Developing new materials through molecular design and surface modification of SRNF membranes for improving comprehensive performance of the membranes in a certain solvent system will be attracted more and more attention in the following years.

Mass Transfer of Polymeric SRNF Membranes

It is imperative to explore the process parameters and investigate the transport mechanism of solutes and solvents through polymeric SRNF membranes to predict the field-specific performance of SRNF membranes. This information will guide the rapid development of polymeric SRNF membranes in dynamic applications. However, building a general model to clarify the mass transfer through SRNF membranes is difficult because the physical and chemical factors that affect the mass transfer process are too complicated. In fact, the literature lacks consensus on the transport mechanism of SRNF, although numerous studies have recently focused on this problem.

To study the transport mechanism of SRNF membranes, clarifying the structure, the changes of structure, and other properties of SRNF membranes is rather significant. FTIR-ATR and XPS are usually applied to characterize the chemical structure of the top surface of the membranes to verify the reaction of the groups or the interaction between different polymer molecules. SEM

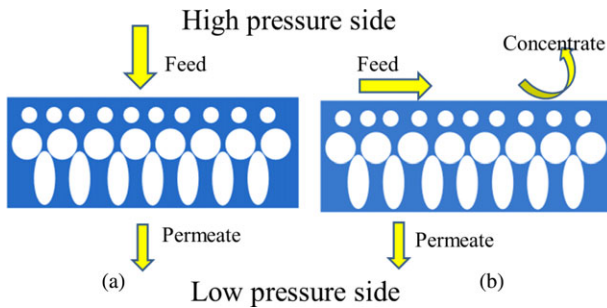


FIGURE 8. Schematic representation of the filtration modes of SRNF membranes: (a) dead-end mode; (b) cross-flow mode.

and AFM are usually used to determine the morphology the membranes. AFM can also be utilized to characterize pore size and pore size distribution of SRNF membranes, although it can not differentiate between surface cavities and active pores contributing to solute transport. Gel content (represents how much a material can be dissolved in a certain solvent) and swelling degree (depicts how much a materials can be swell in a certain solvent) are used to describe the stability of a kind of materials in a certain solvent.

The separation performances of the SRNF membranes are not only due to their basic properties including chemical structure, pore structure, and their stability in a certain solvent but also due to the operation mode. The dead-end filtration mode can be used to test the solvent permeability and rejection of SRNF membranes at the laboratory scale. However, SRNF membranes are typically operated in cross-flow mode at the industrial scale. In dead-end mode (Fig. 8), the feed is forced through SRNF membranes perpendicular to the membrane surface. However, it flows parallel to the membrane surface. Therefore, the polarization concentration tested in the dead-end filtration system increases over the real condition. In dead-end mode, a gas typically provides the pressure difference between the two sides of the membrane, while the driving force is supplied by the kinetic energy of the solution offered by the pump. In fact, most of reported data on solvent flux and rejection were obtained using dead-end testing. The polarization concentration cannot be ignored for long-term dead-end tests. Therefore, cross-flow mode more accurately simulates industrial applications where spiral-wound modules have been used.

The following section will present the main models of solvent permeation through SRNF membranes, including the advantages and disadvantages of every model. Furthermore, the effects of the physical and chemical parameters of solvents, solutes, and membranes on the mass transfer of SRNF membranes will be introduced in detail.

THE SOLVENT TRANSFER MODELS

The Development of Solvent Transfer Models

In essence, two types of mathematical models can describe the solvent (including water) transfer through a SRNF membrane, namely the pore-flow model and the solution-diffusion model. The pore-flow and solution-diffusion models accurately predict the solvent permeability of porous or dense NF membranes, respectively. Nevertheless, the prediction of solvent transfer per-

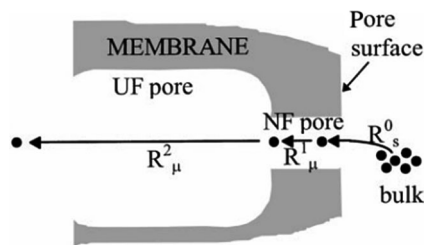


FIGURE 9. Representation of the three flow resistances encountered by a solvent.¹²⁵

formance through SRNF membranes is not consistent with the empirical data due to strong interactions between the solvents and membranes. In this section, the most important and comprehensive models will be introduced to better predict the transfer mechanism of SRNF membranes. Machado et al.¹²⁵ developed a type of resistance-in-series model by combining viscous and diffusion mechanisms. The model successfully predicted the permeability of alcohols, paraffins, acetone, and water through MPF-50, a type of silicone polymeric membrane. This model was based on the assumption that SRNF membranes are composed of three layers (Fig. 9): (a) an active surface skin, (b) an intermediate UF layer, and (c) a base support layer. As the pore size of the membrane decreases, the molecular force at the interface between solvents and membranes increases. Given that the main resistance of every layer affects solvent transfer, the solvent viscous flux through this composite porous membrane can be expressed by Eq. (1):

$$J = \frac{\Delta P}{R_T} = \frac{\Delta P}{R_s^0 + R_\mu^1 + R_\mu^2} \quad (1)$$

where J is the solvent flux, ΔP is the trans-membrane pressure, R_T represents total solvent transfer resistance, R_s^0 stands for the surface resistance at the pore entrance, R_μ^1 is the viscous resistance during the flow through pores in the active surface skin, and R_μ^2 signifies the viscous resistance during flow through the UF portion of the pore. The surface resistance is assumed to be proportional to the difference between the surface tension of the membrane and the solvent as well as $(d_p^1)^2$. This relationship is given below in Eq. (2)^{126,127}:

$$R_s^0 = \frac{k_M^0}{(d_p^1)^2} (\gamma_c - \gamma_L) \quad (2)$$

where k_M^0 is defined as a constant that depends on the pore characteristics of the membrane, d_p^1 represents the mean pore diameter of the active surface skin layer, γ_c stands for the critical surface tension of the membrane as determined by the Zisman plot, and γ_L is the surface tension of the solvent.

The viscous resistance is given by the capillary flow equation:

$$R_\mu^i = k_M^i \frac{\mu}{(d_p^i)^2} \quad (i = 1, 2) \quad (3)$$

where i represents the number of layers, 1 signifies the active surface skin, 2 is defined as the intermediate UF layer, k_M is a

geometric membrane constant determined by the porosity and tortuosity factors, μ stands for the viscosity of the solvent, and d_p^i is the pore size diameter of the different layers of the SRNF membrane. Thus, Eq. (1) can be reorganized into Eq. (4) when considering Eqs. (2) and (3):

$$J = \frac{\Delta P}{\phi[(\gamma_c - \gamma_L) + f_1\mu] + f_2\mu} \quad (4)$$

where $f_1 = k_M^1/k_M^0$ is a solvent-independent parameter that characterizes the active surface skin layer, $f_2 = k_M^2/(d_p^2)^2$ stands for a solvent-independent parameter that characterizes the second UF layer and $\phi = k_M^0/(d_p^1)^2$ is a solvent-dependent parameter.

Because it considers the surface tension difference between the solvent and the membrane, this model can more accurately predict the empirical data than basic models. Understanding the causes of deviations of commonly used models from the empirical solvent permeability data is paramount. Although this model hints at reasons for the failures of the two basic to predict the solvent permeability in nonaqueous media, it is still far from perfect because the effects of solvent polarity and membrane swelling on the solvent transfer through SRNF membranes are not considered.

Bhanushali et al.¹²⁸ presented a valuable model based on the solution-diffusion model. They attributed the deviation of the solution-diffusion to the approximation made by the following equation in the inference process:

$$1 - \exp\left(-\frac{V_i(\Delta P - \Delta\pi)}{RT}\right) = -\frac{V_i(\Delta P - \Delta\pi)}{RT} \quad (5)$$

When considering pure solvents passing through the membrane only, $\Delta\pi$ should be ignored. However, they indicated that the approximation is inaccurate for solvent systems that are well fitted in aqueous systems where the molar volume of water is $18 \text{ cm}^3 \text{ mol}^{-1}$. They then analyzed the possible influencing factor that might result in the deviation based on the solution-diffusion model. Eventually, they stated that the final pure water flux is proportional to the molar volume of solvent (V_m), the reciprocal of viscosity (μ), and the surface energy of the membrane (γ_{SV}):

$$J \propto \left(\frac{V_m}{\mu}\right) \left(\frac{1}{\phi^n \gamma_{SV}}\right) \quad (6)$$

where ϕ is the sorption value representing the interaction between polymer and solvents, and n is an empirical constant. As such, Bhanushali et al.¹²⁸ first clarified the effects of at least three parameters: viscosity, molecular size, and the affinity of the solvent permeability of SRNF membranes. The model correlates well with the experimental data and is the best model available to describe solvent transfer through relatively dense NF-membranes in certain cases. However, this model does not consider swelling effects and thus is not suitable to predict solvent transfer through SRNF membranes that are highly swollen in the given solvent. Another disadvantage of this model is that a higher flux increases the affinity between solvents and membranes, yet the model predicts a decreasing flux.

Geens et al.¹²⁹ and Darvishmanesh et al.²⁴ further amended the model proposed by Bhanushali et al.¹²⁸ Geens et al.¹²⁹ con-

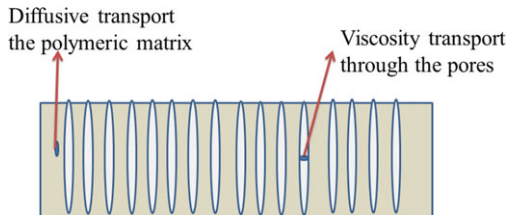


FIGURE 10. Schematic representation of solvent transport through the nanofiltration membrane.²⁴

sidered the effect of membrane–solvent interactions on the resistance. The pure solvent flux was ultimately related to the molar volume of the solvent, the viscosity of the solvent and the surface tension difference between solvents and membranes ($\Delta\gamma$). This relationship is given by Eq. (7):

$$J \propto \left(\frac{V_m}{\mu}\right) \left(\frac{1}{\Delta\gamma}\right) \quad (7)$$

This model correlates well with experimental results and is easily applied because all the necessary parameters can readily be acquired. Furthermore, this model accurately predicts the pure solvent flux through both hydrophilic and hydrophobic membranes. However, the authors also stated that the main disadvantage of the model is that the swelling effects were not included. In addition, the solvent polarity was also excluded and only polar solvents were considered.

Darvishmanesh et al.^{23–25,130} published a series of studies on the solvent transfer mechanism and provided a general model to predict the solvent flux through different membranes. The most important factors that influence the solvent permeability of SRNF membranes are the solvent polarity (dielectric constant), solvent viscosity, solubility parameter, surface tension, and molar volume. As shown in Fig. 10, a semi-empirical model has been developed from the solution-diffusion model and the imperfection model. The membrane is considered a parallel connection of a matrix in which the solution-diffusion mechanism of solvent transfer can occur and the solvent is convectively transferred through pores without changes in concentration. When considering viscous transport through imperfections in the membrane in addition to diffusive transport, the solvent transfer equation can be expressed as follows according to Sherwood et al.¹³¹:

$$J = L_d(\Delta P - \Delta\pi) + L_v\Delta P \quad (8)$$

where J signifies the pure solvent flux, L_d and L_v are new parameters that represent the partial diffusional and viscous permeability (which are related to different factors), ΔP stands for the trans-membrane pressure, and $\Delta\pi$ is the osmotic pressure, which is neglected for pure solvents. The following equation considers the effects of solvent viscosity and surface tension:

$$L_i \propto \frac{1}{\mu \exp(1 - \beta)} \quad (9)$$

where the subscript i represents d or v , μ signifies the solvent viscosity, β stands for the ratio of the surface tension of the membranes, which is defined as:

$$\beta_{\text{hydrophilic}} = \frac{\gamma_L}{\gamma_M} \quad (10)$$

or

$$\beta_{\text{hydrophobic}} = \frac{\gamma_M}{\gamma_L} \quad (11)$$

where γ_M and γ_L are the surface tension of the NF membrane and solvent, respectively.

An additional term related to the diffusive portion in the equation considers the additional effect of polarity. This term is mainly governed by diffusion because the solvent transfers through the dense membrane matrix:

$$L_d \propto \frac{\alpha}{\mu \exp(1 - \beta)} \quad (12)$$

where α is the nondimensional polarity coefficient, which is defined separately for hydrophilic and hydrophobic membranes. For hydrophilic membranes, α is the ratio of the solvent's dielectric constant that of water because water is an extremely polar solvent compared to other solvents and has a high flux through hydrophilic membranes. Similarly, for hydrophobic membranes, α is the ratio of n-hexane's dielectric constant to the solvent's dielectric constant.

Therefore, the final format of Eq. (8) is:

$$J = \frac{a_0 \alpha}{\mu \exp(1 - \beta)} (\Delta P - \Delta \pi) + \frac{b_0}{\mu \exp(1 - \beta)} \Delta P \quad (13)$$

where a_0 and b_0 are the specific diffusivity and permeability values, which can be obtained during modeling. The solvent permeability calculated with the new model correlated well with the experimental data of both hydrophilic and hydrophobic NF membranes over the entire range of solvents used (including both high-polar solvents and apolar solvents), which confirmed that the assumption of convective-diffusive transfer in SRNF membranes is valid. Many other comprehensive models have been proposed, such as the coupled series-parallel resistance model²⁵ as well as mechanistic, chemometric, and hybrid models,¹³² which are not discussed in this review.^{133–135}

The Influencing Factors of Solvent Transfer Through Polymeric SRNF Membranes

Unlike in aqueous solution, the strong interaction between NF membranes and solvent significantly affects the permeability of the solvent. Therefore, the transfer of solvent through SRNF membranes is complex and is influenced by the properties of the solvent, the nature of the membrane, and the interaction between the solvent and the membrane.

Solvent Properties. Polarity, viscosity, surface tension, and the molar volume of solvents are the main factors that determine the behavior of solvent transfer through SRNF membranes. Robinson et al.¹³⁶ found that the solvent polarity was a good estimation of solvent permeability. However, the effect of solvent polarity seemed strongly related to the surface tension,

which may be the intrinsic determining factor. On the other hand, Whu et al.¹³⁷ examined the permeability of MPF-44 membranes to methanol and water (commercial membrane from Koch Membrane System) and claimed that MPF-44 membranes were more permeable to water than methanol permeability because the membrane was hydrophilic. Van der Bruggen et al.¹³⁸ argued that the solvent flux increased for hydrophilic membranes and decreased for hydrophobic membranes when increasing the solvent polarity. Darvishmanesh et al. also found a similar effect. However, in most cases, the effect of surface tension has been intensively addressed, although the surface tension and solvent polarity are intimately related. In fact, the effect of solvent polarity should also be individually considered in addition to the surface tension.^{23–25,130} Compared with the solvent polarity, the solvent viscosity is generally believed to be a predominate factor that affects the solvent permeability.¹³⁹ All of the solvent transfer models mentioned above illustrate that the solvent permeability decreases dramatically with increased the solvent viscosity.^{24,125,128,129} Stamatialis et al.¹⁴⁰ found a valid linear correlation between the solvent permeability and (membrane) swelling/(solvent) viscosity ratio. Vankelecom et al.¹⁴¹ also found similar results. Furthermore, Darvishmanesh et al.^{23,130} indicated that the transfer of solvent through porous SRNF membranes is mainly affected by the solvent viscosity. Machado et al.¹²⁵ attributed the deviation of basic models from the experimental data to the fact that the surface tension difference between solvents and membranes is not considered in these models. The relative surface tension between solvents and membranes determines the interaction between solvents and membranes. In the model developed by Geens et al.,¹²⁹ the solvent permeability was proportional to the reciprocal of the difference in the solvent surface tension. This finding agreed well with the model developed by Machado et al.¹²⁵ The molar volume, which represents the size of the solvent, seems to be a controversial factor that affects the solvent permeability. Bhanushali et al.¹²⁸ and Geens et al.¹²⁹ stated that the solvent flux increased with the solvent molar volume. Nevertheless, Vankelecom et al.¹⁴¹ reported that the solvent molar volume minimally affected the solvent permeability. In fact, the effect of molar volume had been excluded in the models established by Machado et al.¹²⁵ and Darvishmanesh et al.²⁴

Membrane Properties. The membrane properties, including the pore structure (dense or porous) and surface energy, play an important role in determining solvent transfer. For dense membranes, the mutual affinity between solvents and membranes dominated the solvent permeability. On the contrary, the solvent permeability was significantly affected by the viscosity in porous membranes.²⁵ The membrane surface energy is a factor related to the mutual affinity of the used solvents. When the difference between the surface tension of solvents and the surface energy of membranes diminishes, a strong affinity can result in a higher solvent permeability.^{23–25,125,128–130}

The Interaction between Solvents and Membranes. The swelling that results from the strong interaction between solvents and membranes significantly affects the solvent permeability of SRNF membranes. However, this parameter is excluded in most

models.^{24,125,128,129} When polymers swell, the reorganization of the molecular structure of the membrane affects the solvent flux.^{138,142} Extensive swelling can decrease the selectivity and even cause the peeling of the top layer. Many reports have indicated that the solvent permeability was proportional to the swelling/viscosity.^{140,141,143} However, the established models do not accurately correlate the solvent permeability and swelling because the swelling phenomenon is physicochemically complex. Understanding the effects of swelling on the solvent permeability can provide insights into the solvent transfer mechanism. Therefore, this topic requires further exploration in the future.

THE SOLUTE TRANSPORT THROUGH POLYMERIC SRNF MEMBRANES

In a practical SRNF separation process, SRNF membranes necessarily feature a high rejection of a particular solute, which is based different factors of the solute transport. Based on observations made aqueous solutions, the MWCO is an important parameter in the prediction of the rejection of a certain solute in organic solution. However, the MWCO can be inaccurate in this setting for some systems,^{144,145} which indicates that many other important factors can affect the solute transfer through SRNF membranes. Although a consensus solute transport mechanism has not yet been reported, increasing attention has been paid to the investigation of the influencing factors.

The Development of MWCO Characterization

Pore size and pore size distribution are inherent physical factors of SRNF membranes that affect the solute transport. Transmission electron microscope is thought to be a precise technique to characterize the pore structure, however, it is hard to prepare samples and the characterization process is too complex.¹⁴⁶ Therefore, an easily obtainable parameter to reflect the pore size structure in practical applications of SRNF membranes is required. This spurred studies investigating MWCO as such a parameter because MWCO is commonly used to predict the rejection of certain solutes in aqueous solutions. However, the predictions made by MWCO are not always accurate, primarily because the determination of the MWCO of membranes in organic solutions has not been standardized. A standard method should satisfy the following conditions: (a) the used solutes should be readily soluble in a wide range of solvents, (b) the molecular weight of the used solutes should be systematically varied from 200 to 1000 g mol⁻¹, (c) the interaction between the used solutes and membranes as well as between the used solutes and solvents should not be strong. Following these rules, Toh et al.¹⁴⁷ stated that styrene oligomers, which are uncharged, nonpolar, readily detected by UV absorbance, and can be readily dissolved in many solvents ranging from DMA to acetone. With this method, the molecular weight of the solute at which the rejection of SRNF membranes exceeds 99.9% can be examined to indicate the point at which the solutes are completely removed from the solution. However, the main drawback of this method is that the oligostyrene standards are very expensive.¹⁴⁷

To solve this problem, Li et al.¹⁴⁸ focused on using polyethylene glycol as a probe molecule to determine the MWCO of SRNF membranes using high-performance liquid chromatography with an evaporative light scattering detector (ELSD), even though PEGs are typically used to characterize the pore structure of membranes in aqueous solution. They stated that ELSD can be operated using a gradient elution with a low baseline drift to accurately quantify results even at low concentrations. More importantly, ELSD is not affected by the interaction between solvents and solutes. Alkane systems¹⁴⁹ and different dyes¹⁵⁰ have also been used as probe molecules to determine the MWCO of SRNF membranes. However, the drawbacks of alkanes included the lack of commercially available molecules with a molecular weight over 400 g mol⁻¹ and difficulties in detection. The drawbacks of dyes were the strong interaction between the dyes and the membranes because the majority of dyes are charged. Therefore, a standard comprehensive method to examine the MWCO of SRNF membranes remains elusive.

The Crucial Factors of Solute Transport

Although a significant number of studies have focused on solute transport mechanisms, the development of a general model to describe the transfer of solute through SRNF membranes remains a challenge. Therefore, selecting the most suitable membranes and adjusting the filtration conditions (operating pressure, pH value, etc.) to clarify the factors that affect the solute transfer is crucial to design SRNF membranes that perform well in practical applications. The most significant factors that influence the transfer of solutes through SRNF membranes include: (a) the solute properties (molecular size, charges, polarity, etc.); (b) the membrane properties; (c) the interaction between solvents and solutes; and (d) the interaction between solvents and membranes.

Solute Properties. The properties of a solute directly affect the solute permeation through SRNF membranes. According to the sieving effects that play a dominate role and Donnan effects that play a relatively minor role since the ionization of the membranes in solvent environment is not as strong as that in aqueous solution, the molecular size and charge of a certain solute determine whether it passes through the SRNF membrane. For nonelectrolyte solutes, the rejection increases with increasing molecular size. White et al.¹⁴⁹ revealed that branched alkane molecules show a higher rejection than linear alkanes of similar molecular weight. Similar results have been found by Zheng et al.¹⁵¹ and Darvishmanesh et al.¹⁵² Zheng et al. attributed this phenomenon to the fact that molecular weight does not necessarily reflect molecular size. They stated that the "calculated mean size" of solutes based on the 3-D molecular length correlates with the rejection and should be compared with six traditional molecular size descriptors, including different molecular weights and radius of gyration. The solute charge significantly affects the rejection via the electrostatic force between solutes and membranes.¹⁵¹ Darvishmanesh et al.¹⁵² claimed that the molecular structure and electron density of molecules significantly affected the rejection, as predicted by molecular dynamic simulations. They found that molecules with one hydrophilic group showed a lower rejection

resulting from the orientation of the molecule.¹⁵² Li et al.³⁷ reported that membranes showed a higher rejection to dyes with a high valence state charge than mono-charged dyes, a finding that was attributed to the Donnan effects. They also stated that negatively charged PE membranes rejected more MO (a type of negative solute) than positively charged dyes.³⁶ Similar results have been reported in other works¹⁵³ indicating that the Donnan effects may also play an important role in separating charged solutes.

Membrane Properties. The properties of the membrane, including the pore structure, surface charge, and affinity between solutes and membranes, directly affect the solute transfer process. The pore size and pore size distribution of SRNF membranes are affected by the swelling effects of solvents. Furthermore, the effects of the surface charge on the solute permeation can be related to the solute charges, which have been discussed above. Bhanushali et al. examined the rejection of PDMS membranes to Sudan IV in methanol. PDMS membranes showed a negative rejection, and the solute transferred faster than the solvent because of the strong interaction between Sudan IV and PDMS membranes.¹⁵⁴ Darvishmanesh et al.¹⁵⁵ reported a similar phenomenon in determining the rejection of Sudan Black and Sudan 408 in n-hexane by STARMEM™ 122, a type of commercial PI membrane. Therefore, membranes that show a strong affinity for the solute should have a lower rejection.¹⁵⁵

Interactions between Solvents and Solutes. Unlike solute properties and membrane properties, the interactions between solvents and solutes affect the solute transfer process by influencing the solute molecular size via the solvation and hydration of solutes.^{153–157} Bhanushali et al. systematically studied the solute transport through SRNF membranes and stated that the solute-solvent coupling had a significant role in solute permeation.¹⁵⁴ However, further researches are needed to clarify the effects of the interaction between solvents and solutes on the rejection of solutes since some SRNF membranes show negative rejections in certain solvents.^{158,159}

Interactions between Solvents and Membranes. The swelling of SRNF membranes in organic solvents reorganizes the membrane materials resulting in pore structure variations. The swelling of membranes increases the free volume, resulting in lower rejections by dense membranes. Moreover, the rejection increased as the pores narrowed during the swelling of porous membranes (Fig. 11).²³ Geens et al.¹³⁹ examined the rejection of SRNF membranes and found that membrane swelling narrowed the pores of porous membranes. However, some studies have shown that membrane swelling dramatically increased the flux of the solution without obvious changes in the solute rejection.¹⁶⁰ The difference may be caused by the difference of selective layer structure of the SRNF membranes. For the dense membranes, the free volume plays main role in rejecting of solutes, whereas the pores between the selective layer molecules determine the rejections to solutes for the porous membranes. In a word, the swelling effects on the solution transfer through SRNF membranes are a complex process that requires further study.

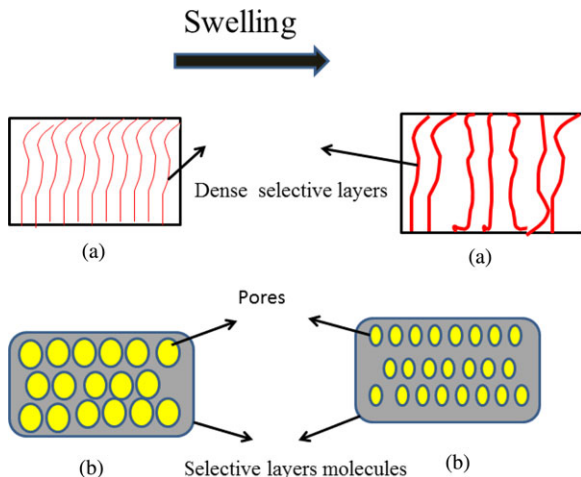


FIGURE 11. The influence of swelling on a dense (a) and a porous (b) membrane.²³

Advanced Applications of SRNF Membranes

As NF has two unique features as talked before, it has been widely applied in many fields, especially in the removal of hazardous contaminates from waste water.^{124,161–164} Most recently, the separation and purification of active molecules in organic medium by NF membranes (called SRNF membranes) has attracted significant attention because unlike conventional distillation, this process is athermal.^{165–168} The SRNF membranes can potentially be used in the pharmaceutical manufacturing industry,^{165–172,198–200} catalysis recovery processes,^{173–183,196,197} the concentration of biologically active compounds in food technology,¹⁹² the recovery of ion liquids,^{184–186} the purification of fuels and solvents,^{188,189} refining technologies,¹⁸⁷ and many other fields.²⁰⁵ All of these fields have a common feature: the cost and the energy consumption to prepare or recover active molecules are very high, which makes the application of SRNF economically attractive. Table II summarizes the characteristics of commercial SRNF membranes. Typical advanced applications of SRNF membranes over the last 10 years will be introduced below.

PHARMACEUTICAL APPLICATIONS

SRNF has three prominent advantages for pharmaceutical applications: (a) it can purify active pharmaceutical ingredients (APIs) without thermal structural damage; (b) it can effectively remove impurities, including some genotoxic and carcinogenic impurities; (c) it reduces energy consumption and recovers a high amount of solvent. Sheth et al.¹⁶⁵ claimed that precompacting commercial MPF-50 or MPF-60 with used solvents at operational pressures and temperatures is necessary to remove erythromycin because precompaction increased the rejection of erythromycin by SRNF membranes, which reduced the loss of erythromycin and increased the purification efficiency. Shi et al.¹⁶⁶ fabricated a type of PI membrane to concentrate spiramycin

TABLE II
Commercial Brands of Solvent-Resistant Nanofiltration Membranes

Trade Name	Manufacturer	Series	Materials Affinity	MWCO (Da)	Stable in	Module Configuration	References
SeIRO®	Koch, USA	MPF-44	Hydrophilic (PDMS based)	250 (glucose in water)	Aqueous mixtures of lower alcohols, hydrocarbons, chlorinated solvents, aromatics, ketones, diethyl ether, EA, cyclohexane, propylene oxide, acetonitrile, THF, 1,4-dioxane, dichloromethane (DCM)	Flat sheet or spiral-wound	165,174,175
		MPF-50	Hydrophobic (PDMS based)	700 (Sudan IV in EA) (Trade off)			165,174
		MPF-60	Hydrophobic (PDMS based)	400 (Sudan IV in acetone) (Trade off)			165,174
StarMem™	W.R. Grace-Davison, USA; Membrane Extraction Technology, UK	StarMem™ 120	Hydrophobic (PI based)	200 (n-alkanes in toluene)	Alcohols, alkanes, aromatics, ethers, ketones, esters, EA, DCM, THF	Flat sheets, pre-cut discs or spiral-wound	169,174,175,182,189
		StarMem™ 122		220 (n-alkanes in toluene)			168-171,173-175,180,182,184,190-192,195,197
		StarMem™ 228		280 (n-alkanes in toluene)			169,179,184,196
		StarMem™ 240		400 (n-alkanes in toluene)			171-175,180,182,184,185,189,196,197
Puramem™		Puramem™ 280	Unknown	280 (styrene oligomers in toluene)	EA	Flat sheet or spiral-wound	170,171
SolSep	SolSep BV, Netherlands	Solsep 030705	Hydrophobic (Unknown material)	Not specified	Methanol, ethanol, propanol, acetone, EA, hexane, toluene, chloro benzene, other alcohols, ketones, esters, DMF, DMSO, THF, etc.		189
		Solsep 030306F NF010206	Hydrophobic (Unknown material)	Not specified			189,195
DuraMem™		DuraMem™ 150	Hydrophobic (Unknown material)	300 (R95%)	Alcohols, esters		167
		DuraMem™ 200	Hydrophobic (Unknown material)	150	Iso-propanol, methanol, EA, ethanol, heptanes		168,171
		DuraMem™ 300	Hydrophobic (modified PI)	200			171
		DuraMem™ 500	Hydrophobic (modified PI)	300			172
GMT-oNF-2	Borsig Membrane Technology GmbH, Germany	GMT-oNF-2	Silicone polymer-based composite type	500	Alkanes, aromatics, alcohols, ethers, ketones		172,196
Desal	GE, USA	Desal-5	Hydrophilic (PA based)	327 (93%)			167
		Desal-5-DK	Hydrophilic (PA based)	350	Methanol, ethanol, EA, DCM, THF		174,175
				200	Methanol, ethanol		185,189,195

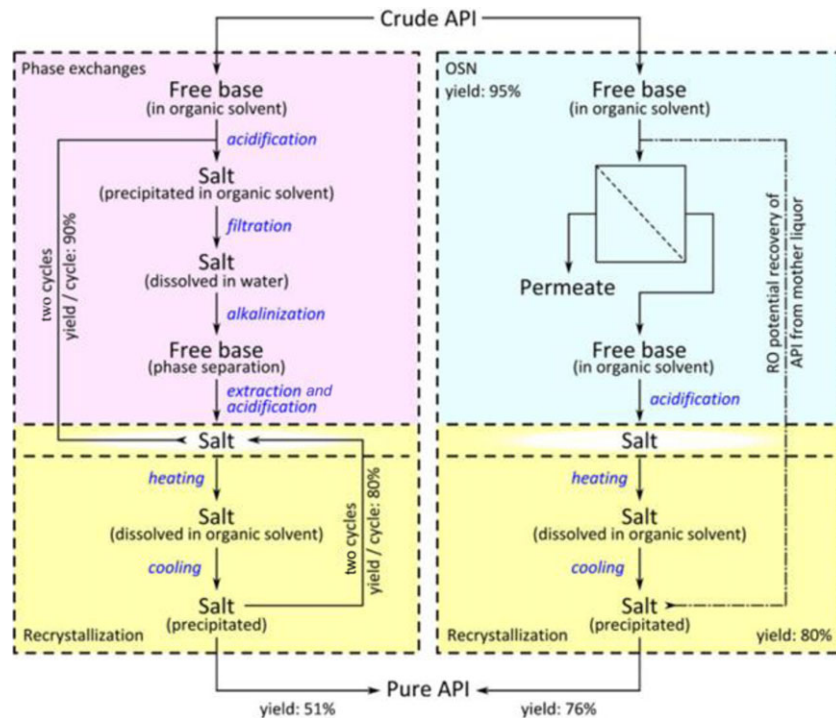


FIGURE 12. Schematic comparison of API purification by a conventional and OSN-based process.¹⁶⁷

TABLE III
The Conditions of the Three Specific Conditions in Separation of API/Genotoxic (GTI) Mixture¹⁶⁷

Cases	API versus GTI	Rejections (%)		Conditions: Membrane, Solvent, Pressure
		API	GTI	
Case 1: Easy	Irb versus ACR	99.3	2.2	GMT-oNF-2, THF, 20
	Meta versus AA	99.2	1.3	SolSep, MEK, 20
Case 2: High GTI rejection	Meta versus DMS	99.1	16.4	SolSep, MEK, 10
Case 3: Low API rejection	Suma versus DMS	99.3	26.4	SolSep, MEK, 20
		95.2	9.3	GMT-oNF-2, THF, 20

extracts and recover the used solvent (butyl acetate). They indicated that the permeability of the spiramycin solution was significantly affected by the operating conditions, although the rejection of spiramycin (higher than 99%) was not influenced.¹⁶⁶

Recently, SRNF membranes for pharmaceutical applications have been systematically and practically studied. Szekely et al.¹⁶⁷ used platform SRNF membranes (Sol Sep) purchased from Borzig Membrane Technology GmbH to remove genotoxic impurities and recover API. The final yield of recovered API by this SRNF process was 25% higher than that of the conventional distillation process (Fig. 12). In addition, they divided different API/genotoxic systems into three categories according to the relative rejection of API and genotoxic impurities. The conditions of the three cases are listed in Table III. Case 1 easily removed genotoxic impurities from API solutions because the rejection of API exceeded 99%. Case 2 and case 3 did not perform as well as case 1 because the rejection of genotoxic impurities was high (over 10%) in case 2 and the rejection of API was approximately 95% in case 3. The loss of API in case 3 was similar to that of

a conventional phase exchange process. The genotoxic impurities could not be completely removed in case 2 although the loss of API was minimal. With respect to safety, the operating conditions must be adjusted to maintain the concentration of genotoxic impurities lower than the maximum limits.

Van der Bruggen and coworkers^{168,169} have studied the purification of API and solvent recovery with SRNF membranes. Initially, they verified that the solvents (IPA, methanol, ethanol and ethylacetate [EA]) and APIs (Imatinib mesylate, Donepezil, Atenolol, Alprazolam and Riluzole) could be recovered and purified using commercial StarMem122 and DuraMem150. DuraMem150 shows very high rejection of all five types of API in all solvent mixtures except IPA. However, StarMem122 showed did not separate Imatinib mesylate in IPA. To prove that this process was feasible on an industrial scale, a model of SRNF membrane units was developed and processed in common simulation software. A comparison between the traditional evaporator process for solvent recovery and the SRNF membrane module confirmed the potential use of SRNF to purify solvents.¹⁶⁸ Another study by

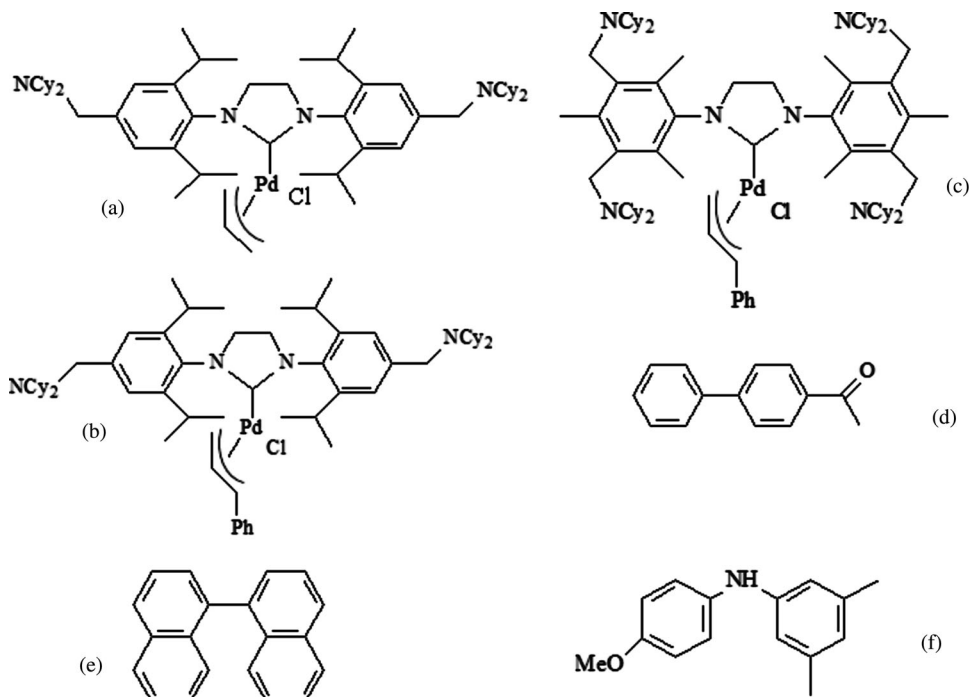


FIGURE 13. Catalysts and products in the Suzuki–Miyaura coupling and the Buchwald–Hartwig amination in literature.¹⁷⁵

the same authors detailed the design of a two-stage membrane process to completely recover API from methanol.¹⁶⁹ In this system, the actual rejection is 91% with an 80% of recovery rate and 83% observed rejection. The continuous separation process yields only 1.7 ppm of API in the permeate solution. Furthermore, the cost of a membrane process was compared to that of a distillation unit. A distillation process that recovers 451 tons of methanol annually consumes 162 MWh, which is over 200 times higher than that the energy consumption of the SRNF separation process.¹⁶⁹ A similar conclusion was made by Rundquist et al.,¹⁷⁰ which indicated that SRNF showed significant potentials for recovering used solvents in the API crystallization process because of its lower energy consumption compared with that of the conventional distillation. Other reports have focused on pharmaceutical purification processes by combining SRNF with other separation techniques, such as counter-current chromatography.¹⁷¹ The concentration of biologically active compounds by the SRNF process has also been studied.¹⁷² Because the SRNF process requires little energy and is athermal (thereby avoiding damage the chemical structure of active molecules), many studies have focused on using SRNF in pharmaceutical fields.

RECOVERY OF CATALYSTS

Similar to pharmaceutical components, catalysts are usually expensive, easily deactivated, and hazardous to the environment and require high energy to be separated from the products using conventional technologies. In fact, catalysts have been applied in almost all chemical synthesis processes, especially in the synthesis of active organic substances or active intermedi-

ates. Because SRNF is an athermal process, which decreases the probability of losing catalyst activity, SRNF membranes could potentially be useful to recover homogeneous or phase transfer catalysts. Luthra et al.^{173,174} successfully used SRNF membranes to recycle phase transfer catalysts. Different commercial SRNF membranes have been used to recycle phase transfer catalysts. A series of commercial STARMEM™ membranes showed the best performance in this process, with a 99% rejection rate and no losses in catalyst activity over a cycle of three consecutive reactions. Most importantly, the concentrated solution can catalyze the reaction in fresh organic reactant solution directly without any further purification or treatment.^{173,174}

Compared with the recovery of phase transfer catalysts, SRNF should be more suitable to recover homogeneous catalysts, especially transition metal catalysts.^{175–183} Schoeps et al.¹⁷⁸ developed a type of PDMS SRNF membrane on a PAN porous support and thermally cross-linked the membranes. This type of thermal cross-linked PDMS/PAN SRNF membrane performed well in Suzuki–Miyaura coupling and Buchwald–Hartwig amination for separating (NHC)Pd(allyl)Cl and (NHC)Pd(cinnamyl)Cl complexes from the coupling compounds (shown in Fig. 13). High rejections ranging from 97% to 99.7% were observed with a 3.5–25 ppm residual content of Pd in the cross-coupling products.¹⁷⁵ Tsoukala et al.¹⁸¹ designed a SRNF process to separate and purify a target product and the Pd catalyst from a Heck coupling post-reaction mixture, shown in Fig. 14. Commercial DuraMem membranes with a MWCO of approximately 200 g mol⁻¹ were most suitable for this purpose. After six filtration cycles, the reaction products were quantitatively recovered and the Pd content in the products was much lower than the requirements illustrated in Fig. 15.¹⁸¹ In

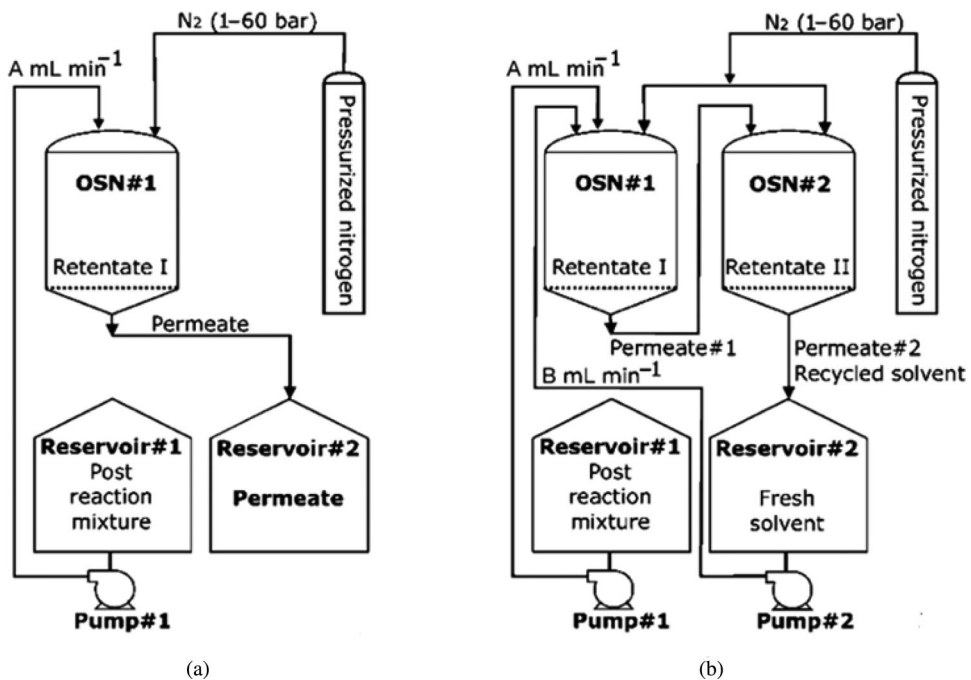


FIGURE 14. (a) Flow diagram for organic solvent dead-end nanofiltration. (b) Organic solvent dia-nanofiltration.¹⁸¹

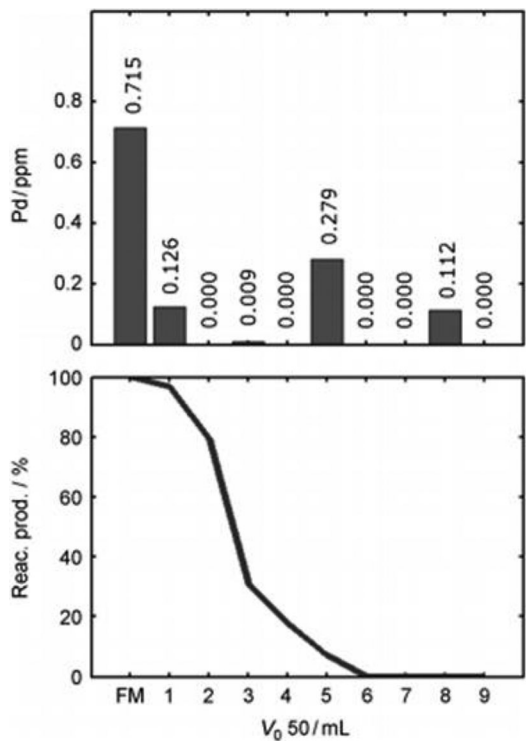


FIGURE 15. Results of the dia-nanofiltration process for the separation of reaction product and catalyst.¹⁸¹

summary, the recovery of catalysts and the purification of organic products by SRNF membranes should be further developed because this process constitutes potential improvements in cost, environmental protection and energy consumption.

OTHER APPLICATIONS

Recently, SRNF processes have attracted the attention of many researchers for purifying, separating, refining and recovering active ingredients in many other fields.^{184,185,187-193,205} Processes that purify ionic liquid are valuable because ionic liquids are expensive and have been widely used to dissolve metal complex catalysts¹⁸⁴ and wooden materials.¹⁸⁵ Han et al.¹⁸⁴ used STARMEM™ membranes to recycle CYPHOS IL 101 ionic liquid from synthetic post-reaction mixtures. The membranes rejected over 95% of the CYPHOS 101 ionic liquid, and the concentration of ionic liquids in the post-reaction mixtures was condensed from 9.1% to 86%. Another interesting study showed that the recovery rates of the ionic liquid in the separation of saccharide products from different feed concentrations of the ionic liquid 1,3-dimethylimidazolium dimethylphosphate can reach 80% by using both Desal series NF membranes and Starmem 240 membranes.¹⁸⁵ Both works illustrate that SRNF separation is potentially very useful to separate ionic liquids.

Many studies have explored the possibility of using SRNF in the conventional chemical separation industry to replace distillation¹⁸⁷⁻¹⁸⁹ and thus reduce energy consumption. White's work¹⁸⁷ developed large-scale applications of SRNF for chemical and refining processes. In these processes, SRNF membranes were applied at the refinery scale to recover solvents (toluene and methyl ethyl ketone) from a lubricant dewaxing process that operated at a feed rate of $5800 \text{ m}^3 \text{ day}^{-1}$. Membrane processes constitute a number of advantages in this setting, including a decrease in energy consumption (20% per unit volume of product), increases in product quality, increased lubricant and wax product yields per barrel of oil and an increased throughput of products. Over 5.3 million dollars could be saved annually by using SRNF for such processes.

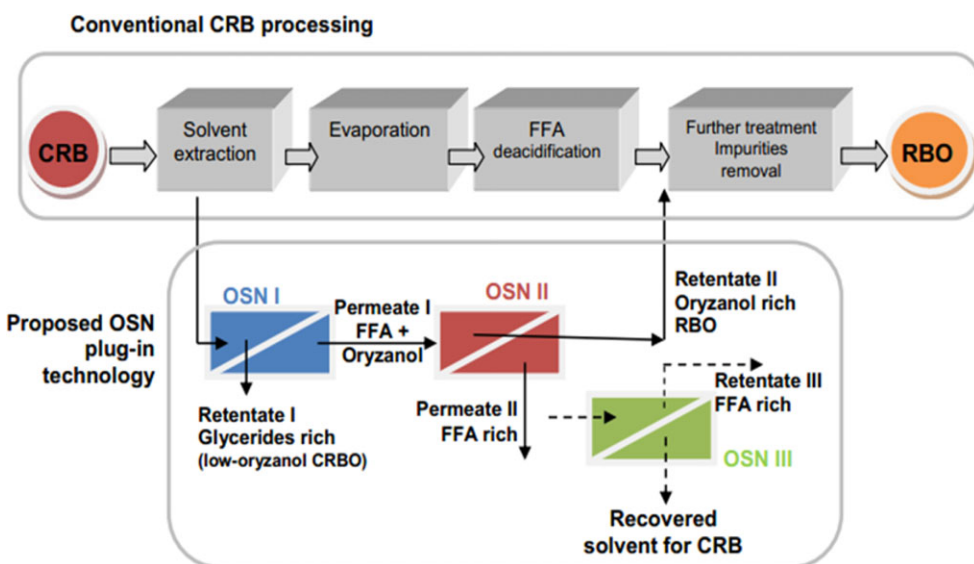


FIGURE 16. Diagram showing conventional CRB processing and how the OSN technology integrates with this conventional process.¹⁹²

SRNF membranes have also been used to purify poly(amidoamine) dendrimers,¹⁹⁰ nutritionally enrich refine food,¹⁹² concentrate dilignols and trilignols from solvent extracts¹⁹³ and serve as a membrane bioreactor unit.¹⁹¹ Among these new application attempts, the work of Sereewatthanawut et al.¹⁹² deserves attention because all retentates and permeates of the SRNF separation process depicted in Fig. 16 are fully utilized. Their results showed an enrichment of γ -oryzanol from 0.95% in the feed oil to 4.1% in the product oil and a more than a twofold increase in the oil antioxidant capacity in conjunction with a considerable nutritional enhancement. In addition, the rice bran oil refining process could be controlled to acceptable levels ($FFA < 0.2$ wt.%) with minimal γ -oryzanol losses, which made the use of SRNF membranes to enrich oil-based products in nutritionally valuable compounds an attractive possibility.¹⁹²

Conclusions and Prospects

The SRNF process has drawn considerable attention in recent years as an alternative separation technique to solve the energy and environmental problems caused by conventional separation methods. Previous studies have investigated the preparation, transport mechanism, and novel applications of SRNF membranes. New materials with various treatment techniques, such as cross-linking, have been developed. The development of new solvent-stable materials, ranging from segmented polymer networks to PIM,^{98–100,102,104,106,108,110,111,114,122,124,207} has provided more possible options for using SRNF membranes at large industrial scales showing the importance of introduction the concept of molecular design in developing new SRNF materials. Mixed matrix membranes and metal–organic frameworks membranes are applied in organic medium as well and will play more and more important role in separation and purification in organic solvent medium since these membranes materials can be designed

form the viewpoint of the structure of selective molecule.^{201,202,208} Besides, based on our most recent study, the addition of various nanoparticles may have great effects on the performance improvement of traditional polymeric SRNF materials.²⁰³ Reductions in the processing cost and environmental contamination have been achieved by decreasing the use of solvents for the conventional cross-linking process by using new techniques, such as UV cross-linking^{54,204}, plasma treatment,⁷¹ and cross-linking in water baths during phase inversion.⁶⁰ In addition, membrane modules, such as capillary and spiral-wound modules,¹¹¹ can potentially be manufactured at the industrial scale.

Numerous studies have attempted to elucidate the transport mechanisms of SRNF membranes. Some studies have focused on developing new characterization methods to clarify the pore size and pore size distribution of SRNF membranes.^{146,206} Others attempt to identify the crucial factors that affect the transport of solvents and solutes through SRNF membranes and build models with which the separation performance can be accurately predicted. With respect to this approach, Darishmanesh and his coworkers have systematically investigated the main factors that affect the permeation of solvents and solution. They built a more suitable model based on the works of Machado et al.¹²⁵ and Bhanushali et al.¹²⁸ to predict the permeation of solvents through SRNF membranes. However, a comprehensive model of the transport of solutes remains elusive because this process is affected by many complex factors. Molecular simulation is a powerful technique that shows promise for making such predictions in the future.

Cost-effective and solvent-stable materials for the fabrication of SRNF membranes should be further developed decrease membrane cost. Advanced cross-linking methods such as the visible light cross-linking strategy deserve more attention. In the following years, the concept of molecular design will play more and more important role in developing new SRNF materials. Furthermore, because the interactions between solutes and membranes significantly affect SRNF performance, it is possible to modify SRNF membranes using well-organized functional

groups with a specific stereoscopic structure to separate and purify specific molecules, such as chiral molecules. Self-assembly techniques prevailing in molecule design provide a possible approach to meet such a target. In a word, the research direction of SRNF materials is undergoing a change from how to broaden the applications of the developed materials to how to obtain the unique separation performance through molecular design or surface modification techniques. Although the SRNF process consumes less energy than conventional separation techniques, it still requires considerable amounts energy when operated at relatively high pressures. Therefore, the development of low-pressure-driven SRNF should be the long-term goal of future research.

Because of the complexities in the process, previous studies have not yet developed a consensus mass transfer mechanism for SRNF membranes. Among the crucial influencing factors, swelling presents the most uncertainties. Swelling can decrease or increase the permeation and MWCO of SRNF membranes depending on the membrane properties. Therefore, building a model with which the performance of different types of SRNF membranes can be exactly predicted is difficult. Although molecular simulations and mechanistic analyses published by Darishmanesh et al.^{152,155} and Santos et al.,¹³² respectively, offer insight into a likely general model, most existing models have excluded swelling effects. Thus, seeking a parameter, such as an interaction parameter between solvents and membranes, to represent the effects of swelling on the separation performance of SRNF membranes is important for building a general model because the swelling of SRNF membranes reorganizes the pore structure of the active layers in the membranes.

Most recently, numerous studies have concentrated on developing new applications for SRNF, especially in high value-added fields, such as the purification of APIs and the recovery of organic metal catalysts. These studies are clearly valuable, but SRNF could also be potentially used in other practical industrial production processes. The field-specific design of membrane modules and membrane processes is also important. The design of membrane processes, which includes the piping design, pump selection, and determination of operating conditions (e.g., flow rate of the feed, trans-membrane pressure, working temperature, and flushing time) considerably influences the final cost of the SRNF process. Moreover, the running cost of the SRNF process is needed to compare it with the conventional separating process before it can be readily applied in industry.

In summary, SRNF membranes have been significantly improved in recent years and future studies should focus on practical issues. These issues include the development of new materials and new approaches to fabricate SRNF membranes, the application of SRNF membranes to separate and purify active substances at industrial scales and the reduction of the running cost of the general process from both economic and environmental perspectives.

Acknowledgments

The manuscript was written through contributions of all authors. All authors have given approval to the final version of the manuscript. The authors declare no competing financial interest.

References

- Shao, L.; Wang, Z. X.; Zhang, Y. L.; Jiang, Z. X.; Liu, Y. Y. *J Membr Sci* 2014, 461, 10–21.
- Xiao, Y. C.; Low B. T.; Hosseini, S. S.; Chung, T. S.; Paul, D. R. *Prog Polym Sci* 2009, 34, 561–580.
- Jung, C. H.; Lee, J. E.; Han, S. H.; Park, H. B.; Lee, Y. M. *J Membr Sci* 2010, 350, 301–309.
- Xu, J.; Feng, X. S.; Gao C. *J Membr Sci* 2011, 370, 116–123.
- Xu, L.; Du, L. S.; Wang, C.; Xu, W. *J Membr Sci* 2012, 409, 329–334.
- Shao, L.; Cheng, X. Q.; Liu, Y.; Quan, S.; Ma, J.; Zhao, S. Z.; Wang, K. Y. *J Membr Sci* 2013, 430, 96–105.
- Wang, K. Y.; Chung, T. S.; Rajagopalan, R. *Ind Eng Chem Res* 2007, 46, 1572–1577.
- Shao, L.; Low, B. T.; Chung, T. S.; Greenberg, A. R. *J Membr Sci* 2009, 327, 18–31.
- Kovacs, Z.; Samhaber, W. *Desalination* 2009, 240, 78–88.
- Yang, Q.; Hu, Y. J.; Xue, L. *Adv Mater Res* 2011, 168–170, 404–407.
- Zhang, Y. M.; Pagilla, K. *Desalination* 2010, 263, 36–44.
- Comes, S.; Cavaco, S. A.; Quina, M. J.; Gando-Ferreira, L. M. *Desalination* 2010, 254, 80–89.
- Religa, P.; Kowalik, A.; Gierycz, P. *J Hazard Mater* 2011, 186, 288–292.
- Zhong, P. S.; Widjojo, N.; Chung, T. S.; Webe, M.; Maletzko, C. *J Membr Sci* 2012, 417, 52–60.
- Aouni, A.; Fersi, C.; Cuartas-Uribe, B.; Bes-Pia, A.; Alcaina-Miranda, M. I.; Dhahbi, M. *Desalination* 2012, 297, 87–96.
- Lee, S.; Lee, C. H. *Water Res* 2000, 34, 3854–3866.
- Schmidt, M.; Mirza, S.; Schubert, R.; Rodicker, H.; Kattanek, S.; Malisz, J. *Chem Ing Tech* 1999, 71, 199–206.
- Vandezande, P.; Gevers, L. E. M.; Vankelecom, I. F. J. *Chem Soc Rev* 2008, 37, 365–405.
- Soroko, I.; Lopes, M. P.; Livingston, A. *J Membr Sci* 2011, 381, 152–162.
- Soroko, I.; Makowski, M.; Spill, F.; Livingston, A. *J Membr Sci* 2011, 381, 163–171.
- Soroko, I.; Sairam, M.; Livingston, A. *J Membr Sci* 2011, 381, 172–182.
- Soroko, I.; Bhole, Y.; Livingston, A. *Green Chem* 2011, 13, 162–168.
- Darvishmanesh, S.; Degreve, J.; Van der Bruggen, B. *Chem Eng Sci* 2009, 64, 3914–3927.
- Darvishmanesh, S.; Buekenhoudt, A.; Degreve, J.; Van der Bruggen, B. *J Membr Sci* 2009, 334, 43–49.
- Darvishmanesh, S.; Buekenhoudt, A.; Degreve, J.; Van der Bruggen, B. *Sep Purif Technol* 2009, 70, 46–52.
- Ulbricht, M., *Adv Funct Polym Membr Polym* 2006, 47, 2217–2262.
- Kim, I. C.; Jegal, J.; Lee, K. H. *J Polym Sci Part B Polym Phys* 2002, 40, 2151–2163.
- Kosaraju, P. B.; Sirkar, K. K. *J Membr Sci* 2008, 321, 155–161.
- Roy, S.; Ntim, S. A.; Mitra, S.; Sirkar, K. K. *Membr Sci* 2011, 375.
- Solomon, M. F. J.; Bhole, Y.; Livingston, A. G. *J Membr Sci* 2012, 423–424, 371–382.
- Solomon, M. F. J.; Bhole, Y.; Livingston, A. G. *J Membr Sci* 2013, 434, 193–203.
- Peng, J.; Su, Y.; Chen, W.; Zhao, X.; Jiang, Z.; Dong, Y. A.; Zhang, Y.; Liu, J. Z.; Cao, X. Z. *J Membr Sci* 2013, 427, 92–100.
- Ahmadiannamini, P.; Li, X. F.; Goyens, W.; Joseph, N.; Meesschaert, B.; Vankelecom, I. F. J. *Membr Sci* 2012, 394, 98–106.
- Ahmadiannamini, P.; Li, X. F.; Goyens, W.; Meesschaert, B.; Vankelecom, I. F. J. *Membr Sci* 2010, 360, 250–258.
- Ahmadiannamini, P.; Li, X. F.; Goyens, W.; Meesschaert, B.; Vanderlinden, W.; De Feyter, S.; Vankelecom, I. F. J. *J Membr Sci* 2012, 403, 216–226.
- Li, X. F.; De Feyter, S.; Chen, D. J.; Aldea, S.; Vandezande, P.; Du Prez, F.; Vankelecom, I. F. J. *Chem Mater* 2008, 20, 3876–3883.
- Li, X. F.; Goyens, W.; Ahmadiannamini, P.; Vanderlinden, W.; De Feyter, S.; Vankelecom, I. F. J. *Membr Sci* 2010, 358, 150–157.

38. Abed, M. R. M.; Kumbharkar, S. C.; Groth, A. M.; Li, K. *J Membr Sci* 2012, 407, 145–154.
39. Gao, L.; Tang, B. B.; Wu, P. Y. *J Membr Sci* 2009, 326, 168–177.
40. Savojo, H.; Rana, D.; Matsuura, T.; Soltanieh, M.; Tabe, S. *J Appl Polym Sci* 2012, 124, 2287–2299.
41. Jansen, J. C.; Macchione, M.; Oliviero, C.; Mendichi, R.; Ranieri, G. A.; Drioli, E. *Polymer* 2005, 46, 11366–11379.
42. Liu, J. Q.; Xu, Z. L.; Li, X. H.; Zhang, Y.; Zhou, Y.; Wang, Z. X.; Wang, X. *J Sep Purif Technol* 2007, 58, 53–60.
43. Verissimo, S.; Peinemann, K. V.; Bordado, J. *J Membr Sci* 2005, 264, 48–55.
44. Fadhillah, F.; Zaidi, S. M. J.; Khan, Z.; Khaled, M.; Hammond, P. T. *Desalin Water Treat* 2011, 34, 44–49.
45. Ge, Q. C.; Wang, P.; Wan, C. F.; Chung, T. S. *Environ Sci Technol* 2012, 46, 6236–6243.
46. Vanherck, K.; Cano-Odena, A.; Koeckelberghs, G.; Dedroog, T.; Vankelecom, I. F. *J Membr Sci* 2010, 353, 135–143.
47. Toh, Y. H. S.; Lim, F. W.; Livingston, A. *J Membr Sci* 2007, 301, 3–10.
48. Shao, L.; Chung, T. S.; Goh, S. H.; Pramoda, K. P. *J Membr Sci* 2004, 238, 153–163.
49. Shao, L.; Liu, L.; Cheng, S. X.; Huang, Y. D.; Ma, J. *J Membr Sci* 2008, 312, 174–85.
50. Jiang, L. Y.; Wang, Y.; Chung, T. S.; Qiao, X. Y.; Lai, J. Y. *Prog Polym Sci* 2009, 34, 1135–1160.
51. Yang, Q.; Chung, T. S.; Xiao, Y. C.; Wang, K. Y. *Chem Eng Sci* 2007, 62, 1721–1729.
52. Toh, Y. H. S.; Silva, M.; Livingston, A. *J Membr Sci* 2008, 324, 220–232.
53. Fang, B.; Pan, K.; Meng, Q. H.; Cao, B. *Polym Int* 2012, 61, 111–117.
54. Park, H. B.; Lee, C. H.; Sohn, J. Y.; Lee, Y. M.; Freeman, B. D.; Kim, H. J. *J Membr Sci* 2006, 285, 432–443.
55. Vanherck, K.; Vandezande, P.; Aldea, S. O.; Vankelecom, I. F. *J Membr Sci* 2008, 320, 468–476.
56. Dutczak, S. M.; Cuperus, F. P.; Wessling, M.; Stamatialis, D. F. *Sep Purif Technol* 2013, 102, 142–146.
57. Vandezande, P.; Li, X. F.; Gevers, L. E. M.; Vankelecom, I. F. *J Membr Sci* 2009, 330, 307–318.
58. Vandezande, P.; Gevers, L. E. M.; Jacobs, P. A.; Vankelecom, I. F. *J Sep Purif Technol* 2009, 66, 104–110.
59. Vanherck, K.; Vankelecom, I.; Verbiest, T. *Membr Sci* 2011, 373, 5–13.
60. Hendrix, K.; Vanherck, K.; Vankelecom, I. F. *J Membr Sci* 2012, 421, 15–24.
61. Valadez-Blanco, R.; Livingston, A. *J Membr Sci* 2009, 326, 332–342.
62. Kim, I. C.; Yoon, H. G.; Lee, K. H. *J Appl Polym Sci* 2002, 84, 1300–1307.
63. See-Toh, Y. H.; Ferreira, F. C.; Livingston, A. *J Membr Sci* 2007, 299, 236–250.
64. Merkel, T. C.; Bondar, V. I.; Nagai, K.; Freeman, B. D.; Pinnau, I. *J Polym Sci Part B Polym Phys* 2000, 38, 415–434.
65. Reijerkerk, S. R.; Knoef, M. H.; Nijmeijer, K.; Wessling, M. *J Membr Sci* 2010, 352, 126–135.
66. Liu, G. P.; Xiangli, F. J.; Wei, W.; Liu, S. N.; Jin, W. Q. *Chem Eng J* 2011, 174, 495–503.
67. Ebert, K.; Koll, J.; Dijkstra, M. F. J.; Eggers, M. *J Membr Sci* 2006, 285, 75–80.
68. Dutczak, S. M.; Luiten-Olieman, M. W. J.; Zwijnenberg, H. J.; Bolhuis-Versteeg, L. A. M.; Winnubst, L.; Hempenius, M. A.; Benes, N. E.; Wessling, M.; Stamatialis, D. *Membr Sci* 2011, 372, 182–190.
69. Gevers, L. E. M.; Vankelecom, I. F. J.; Jacobs, P. A. *Chem Commun* 2005, 19, 2500–2502.
70. Gevers, L. E. M.; Aldea, S.; Vankelecom, I. F. J.; Jacobs, P. A. *J Membr Sci* 2006, 81, 741–746.
71. Aerts, S.; Vanhulsel, A.; Buekenhoudt, A.; Weyten, H.; Kuypers, S.; Chen, H.; Bryjak, M.; Gevers, L. E. M.; Vankelecom, I. F. J.; Jacobs, P. A. *J Membr Sci* 2006, 275, 212–219.
72. Tarleton, E. S.; Robinson, J. P.; Salman, M. *J Membr Sci* 2006, 280, 442–451.
73. Zhao, Y. Y.; Yuan, Q. P. *J Membr Sci* 2006, 280, 195–201.
74. Ben Soltane, H.; Roizard, D.; Favre, E. *J Membr Sci* 2013, 435, 110–119.
75. Li, Y.; Verbiest, T.; Vankelecom, I. F. *J Membr Sci* 2013, 428, 63–69.
76. Ogieglo, W.; van der Werf, H.; Tempelman, K.; Wormeester, H.; Wessling, M.; Nijmeijer, A.; Benes, N. E. *J Membr Sci* 2013, 431, 233–243.
77. Zeidler, S.; Kaetzel, U.; Kreis, P. *J Membr Sci* 2013, 429, 295–303.
78. Zhang, H. Q.; Zhang, Y. J.; Li, L. B.; Zhao, S.; Ni, H. O.; Cao, S. K.; Wang, J. T. *Chem Eng Sci* 2014, 106, 157–166.
79. Oh, N. W.; Jegal, J.; Lee, K. H. *J Appl Polym Sci* 2001, 80, 2729–2736.
80. Korikov, A. P.; Sirkar, K. K. *J Membr Sci* 2005, 246, 27–37.
81. Ladam, G.; Schaaf, P.; Voegel, J. C.; Schaaf, P.; Decher, G.; Cuisinier, F. *Langmuir* 2000, 16, 1249–1255.
82. Liu, X. Y.; Bruening, M. L. *Chem Mater* 2004, 16, 351–357.
83. Stanton, B. W.; Harris, J. J.; Miller, M. D.; Bruening, M. L. *Langmuir* 2003, 19, 7038–7042.
84. Shan, W. Q.; Bacchin, P.; Aimar, P.; Bruening, M. L.; Tarabara, V. V. *J Membr Sci* 2010, 349, 268–278.
85. Malaisamy, R.; Talla-Nwafo, A.; Jones, K. L. *Sep Purif Technol* 2011, 77, 367–374.
86. Ji, Y. L.; An, Q. F.; Zhao, Q.; Chen, H. L.; Qian, J. W.; Gao, C. J. *J Membr Sci* 2010, 357, 80–89.
87. Miller, M. D.; Bruening, M. L. *Langmuir* 2004, 20, 11545–11551.
88. El-Hashani, A.; Toutianoush, A.; Tieke, B. *J Membr Sci* 2008, 318, 65–70.
89. Bruening, M. L.; Dotzauer, D. M.; Jain, P.; Ouyang, L.; Baker, G. L. *Langmuir* 2008, 24, 7663–7673.
90. Hong, S. U.; Malaisamy, R.; Bruening, M. L. *Langmuir* 2007, 23, 1716–1722.
91. Hong, S. U.; Lu, O. Y.; Bruening, M. L. *J Membr Sci* 2009, 327, 2–5.
92. Laschewsky, A.; Wischerhoff, E.; Kauranen, M.; Persoons, A. *Macromolecules* 1997, 30, 8304–8309.
93. Shiratori, S. S.; Rubner, M. F. *Macromolecules* 2000, 33, 4213–4219.
94. Park, S. Y.; Barrett, C. J.; Rubner, M. F.; Mayes, A. M. *Macromolecules* 2001, 34, 3384–3388.
95. Schonhoff, M. *J Phys Condens Matter* 2003, 15, R1781–R1808.
96. Klitzing, R. *Phys Chem Chem Phys* 2006, 8, 5012–5033.
97. Cui, Y.; Wang, H.; Wang, H.; Chung, T. S. *Chem Eng Sci* 2013, 101, 13–26.
98. Volkov, A. V.; Stamatialis, D. F.; Khotimsky, V. S.; Volkov, V. V.; Wessling, M.; Plate, N. A. *J Membr Sci* 2006, 281, 351–357.
99. Volkov, A. V.; Stamatialis, D. F.; Khotimsky, V. S.; Volkov, V. V.; Wessling, M.; Plate, N. A. *Desalination* 2006, 199, 251–252.
100. Volkov, A. V.; Parashchuk, V. V.; Stamatialis, D. F.; Khotimsky, V. S.; Volkov, V. V.; Wessling, M. *J Membr Sci* 2009, 333, 88–93.
101. Volkov, A. V.; Tsarkov, S. E.; Gokzhaev, M. B.; Bondarenko, G. N.; Legkov, S. A.; Kukushkina, Y. A.; Volkov, V. V. *Pet Chem* 2013, 52, 598–608.
102. Fritsch, D.; Merten, P.; Heinrich, K.; Lazar, M.; Priske, M. *J Membr Sci* 2012, 401, 222–231.
103. Tsarkov, S.; Khotimskiy, V.; Budd, P. M.; Volkov, V.; Kukushkina, J.; Volkov, A. *J Membr Sci* 2012, 423, 65–72.
104. Li, X. F.; Vandezande, P.; Vankelecom, I. F. *J Membr Sci* 2008, 320, 143–150.
105. Florian, E.; Modesti, M.; Ulbricht, M. *Ind Eng Chem Res* 2007, 46, 4891–4899.
106. Yan, C.; Zhang, S. H.; Yang, D. L.; Jian, X. G. *J Appl Polym Sci* 2008, 107, 1809–1816.
107. Buonomenna, M. G.; Golemme, G.; Jansen, J. C.; Choi, S. H. *J Membr Sci* 2011, 368, 144–149.
108. Darvishmanesh, S.; Tasselli, F.; Jansen, J. C.; Tocci, E.; Bazzarelli, F.; Bernardo, P.; Luis, P.; Degreve, J.; Drioli, E.; Van der Bruggen, B. *J Membr Sci* 2011, 384, 89–96.
109. Darvishmanesh, S.; Jansen, J. C.; Tasselli, F.; Tocci, E.; Luis, P.; Degreve, J.; Drioli, E.; Van der Bruggen, B. *J Membr Sci* 2011, 379, 60–68.
110. Sairam, M.; Loh, X. X.; Li, K.; Bismarck, A.; Steinke, J. H. G.; Livingston, A. *J Membr Sci* 2009, 330, 166–174.
111. Sairam, M.; Loh, X. X.; Bhole, Y.; Sereewatthanawut, I.; Li, K.; Bismarck, A.; Steinke, J. H. G.; Livingston, A. *J Membr Sci* 2010, 349, 123–129.
112. Loh, X. X.; Sairam, M.; Steinke, J. H. G.; Livingston, A.; Bismarck, A.; Li, K. *Chem Commun* 2008, 47, 6324–6326.
113. Loh, X. X.; Sairam, M.; Bismarck, A.; Steinke, J. H. G.; Livingston, A. *J Membr Sci* 2009, 326, 635–642.

114. Li, X. F.; Basko, M.; Du Prez, F.; Vankelecom, I. F. J. *J Phys Chem B* 2008, 112, 16539–16545.
115. Valtcheva, I. B.; Kumbharkar, S. C.; Kim, J. F.; Bhole, Y.; Livingston, A. G. *J Membr Sci* 2014, 457, 62–72.
116. Xing, D. Y.; Chan, S. Y.; Chung, T. S. *Green Chem* 2014, 16, 1383–1392.
117. Hendrix, K.; Van Eynde, M.; Koeckelberghs, G.; Vankelecom, I. F. J. *J Membr Sci* 2013, 447, 212–221.
118. Hendrix, K.; Koeckelberghs, G.; Vankelecom, I. F. J. *J Membr Sci* 2014, 452, 241–252.
119. Holda, A. K.; Aernouts, B.; Saeys, W.; Vankelecom, I. F. J. *J Membr Sci* 2013, 442, 196–205.
120. Holda, A. K.; Vankelecom, I. F. J. *J Membr Sci* 2014, 450, 512–521.
121. Holda, A. K.; Vankelecom, I. F. J. *J Membr Sci* 2014, 450, 499–511.
122. Tsuru, T.; Nakasui, T.; Oka, M.; Kanazashi, M.; Yoshioka, T. *J Membr Sci* 2011, 384, 149–156.
123. Peyravi, M.; Jahanshahi, M.; Rahimpour, A.; Javadi, A.; Hajavi, S. *Chem Eng J* 2014, 241, 155–166.
124. Zhang, Y.; Su, Y. L.; Chen, W. J.; Peng, J. M.; Dong, Y. A.; Jiang, Z. Y. *Ind Eng Chem Res* 2011, 50, 4678–4685.
125. Machado, D. R.; Hasson, D.; Semiat, R. *J Membr Sci* 2000, 166, 63–69.
126. Israelachvili, J. N. *Intermolecular and Surface Forces*; Academic Press: London, 2011.
127. Zeman, L. J.; Zydney, A. L. *Microfiltration and Ultrafiltration – Principles and Applications*; Marcel Dekker: New York, 1996.
128. Bhanushali, D.; Kloos, S.; Kurth, C.; Bhattacharyya, D. *J Membr Sci* 2001, 189, 1–21.
129. Geens, J.; Van der Bruggen, B.; Vandecasteele, C. *Sep Purif Technol* 2006, 48, 255–263.
130. Darvishmanesh, S.; Degreve, J.; Van der Bruggen, B. *Chem Phys Chem* 2010, 11, 404–411.
131. Sherwood, T. K.; Brian, P. L. T.; Fisher, R. E. *Ind Eng Chem Fundam* 1967, 6, 2–12.
132. Santos, J. L. C.; Hidalgo, A. M.; Oliveira, R.; Velizarov, S.; Crespo, J. G. *J Membr Sci* 2007, 300, 191–204.
133. Fierro, D.; Boschetti-de-Fierro, A.; Abetz, V. *J Membr Sci* 2012, 413, 91–101.
134. Hesse, L.; Micovic, J.; Schmidt, P.; Gorak, A.; Sadowski, G. *J Membr Sci* 2013, 428, 554–561.
135. Leitner, L.; Harsooat-Schiavo, C.; Vallières, C. *Polym Test* 2014, 33, 88–96.
136. Robinson, J. P.; Tarleton, E. S.; Millington, C. R.; Nijmeijer, A. *J Membr Sci* 2004, 230, 29–37.
137. Whu, J. A.; Baltzis, B. C.; Sirkar, K. K. *J Membr Sci* 2000, 170, 159–172.
138. Van der Bruggen, B.; Geens, J.; Vandecasteele, C. *Sep Sci Technol* 2002, 37, 783–797.
139. Geens, J.; Peeters, K.; Van der Bruggen, B.; Vandecasteele, C. *J Membr Sci* 2005, 255, 255–264.
140. Stamatialis, D. F.; Stafie, N.; Buadu, K.; Hempenius, M.; Wessling, M. *J Membr Sci* 2006, 279, 424–433.
141. Vankelecom, I. F. J.; De Smet, K.; Gevers, L. E. M.; Livingston, A.; Nair, D.; Aerts, S.; Kuypers, S.; Jacobs, P. A. *J Membr Sci* 2004, 231, 99–108.
142. Darvishmanesh, S.; Degreve, J.; Van der Bruggen, B. *Ind Eng Chem Res* 2010, 49, 9330–9338.
143. Dobrak-Van Berlo, A.; Vankelecom, I. F. J.; Van der Bruggen, B. *J Membr Sci* 2011, 374, 138–149.
144. Zhao, Y. Y.; Yuan, Q. P. *J Membr Sci* 2006, 279, 453–458.
145. Patterson, D. A.; Lau, L. Y.; Roengpithaya, C.; Gibbins, E. J.; Livingston, A. *Desalination* 2008, 218, 248–256.
146. Stawikowska, J.; Livingston, A. *J Membr Sci* 2012, 413, 1–16.
147. Toh, Y. H. S.; Loh, X. X.; Li, K.; Bismarck, A.; Livingston, A. *J Membr Sci* 2007, 291, 120–125.
148. Li, X.; Monsuur, F.; Denoulet, B.; Dobrak, A.; Vandecasteele, P.; Vankelecom, I. F. *J. Anal Chem* 2009, 81, 1801–1809.
149. White, L. S. *J Membr Sci* 2002, 205, 191–202.
150. Yang, X. J.; Livingston, A.; dos Santos, L. F. *J Membr Sci* 2001, 190, 45–55.
151. Zheng, F. Z.; Li, C. X.; Yuan, Q. P.; Vriesekoop, F. *J Membr Sci* 2008, 318, 114–122.
152. Darvishmanesh, S.; Vanneste, J.; Tocci, E.; Jansen, J.; Tasseli, F.; Degreve, J.; Drioli, E.; Van der Bruggen, B. *J Phys Chem B* 2011, 115, 14507–14517.
153. Geens, J.; Hillen, A.; Bettens, B.; Van der Bruggen, B.; Vandecasteele, C. *J Chem Technol Biot* 2005, 80, 1371–1377.
154. Bhanushali, D.; Kloos, S.; Bhattacharyya, D. *J Membr Sci* 2002, 208, 343–359.
155. Darvishmanesh, S.; Degreve, J.; Van der Bruggen, B. *Phys Chem Chem Phys* 2010, 12, 13333–13342.
156. Gevers, L. E. M.; Meyen, G.; De Smet, K.; De Velde, P. V.; Du Prez, F.; Vankelecom, I. F. J.; Jacobs, P. A. *J Membr Sci* 2006, 274, 173–182.
157. Zwijnenberg, H. J.; Dutczak, S. M.; Boerrigter, M. E.; Hempenius, M. A.; Luiten-Olieman, M. W. J.; Benes, N. E.; Wessling, M.; Stamatialis, D. *J Membr Sci* 2012, 390, 211–217.
158. Postel, S.; Spalding, G.; Chirnside, M.; Wessling, M. *J Membr Sci* 2013, 447, 57–65.
159. Volkov, A.; Yushkin, A.; Kachula, Y.; Khotimsky, V.; Volkov, V. *Sep Purif Technol* 2014, 124, 43–48.
160. Tarleton, E. S.; Robinson, J. P.; Millington, C. R.; Nijmeijer, A.; Taylor, M. L. *J Membr Sci* 2006, 278, 318–327.
161. Chaudhari, L. B.; Murthy, Z. V. P. *J Hazard Mater* 2010, 180, 309–315.
162. Benitez, F. J.; Acero, J. L.; Leal, A. I.; Gonzalez, M. *J Hazard Mater* 2009, 162, 1438–1445.
163. Geise, G. M.; Lee, H. S.; Miller, D. J.; Freeman, B. D.; McGrath, J. E.; Paul, D. *R. J Polym Sci Part B Polym Phys* 2010, 48, 1685–1718.
164. Lu, X. J.; Liu, L.; Liu, R. R.; Chen, J. H. *Desalination* 2010, 258, 229–232.
165. Sheth, J. P.; Qin, Y. J.; Sirkar, K. K.; Baltzis, B. C. *J Membr Sci* 2003, 211, 251–261.
166. Shi, D. Q.; Kong, Y.; Yu, J. X.; Wang, Y. F.; Yang, J. R. *Desalination* 2006, 191, 309–317.
167. Szekely, G.; Bandarra, J.; Heggie, W.; Sellergren, B.; Ferreira, F. C. *J Membr Sci* 2011, 381, 21–33.
168. Darvishmanesh, S.; Firoozpour, L.; Vanneste, J.; Luis, P.; Degreve, J.; Van der Bruggen, B. *Green Chem* 2011, 13, 3476–3483.
169. Geens, J.; De Witte, B.; Van der Bruggen, B. *Sep Sci Technol* 2007, 42, 2435–2449.
170. Rundquist, E. M.; Pink, C. J.; Livingston, A. *Green Chem* 2012, 14, 2197–2205.
171. Rundquist, E.; Pink, C.; Vilminot, E.; Livingston, A. *J Chromatogr A* 2012, 1229, 156–163.
172. Tykłowski, B.; Tsibranska, I.; Kochanow, R.; Peev, G.; Giamberini, M. *Food Bioprod Process* 2011, 89, 307–314.
173. Luthra, S. S.; Yang, X. J.; dos Santos, L. M. F.; White, L. S.; Livingston, A. *Chem Commun* 2001, 16, 1468–1469.
174. Luthra, S. S.; Yang, X. J.; dos Santos, L. M. F.; White, L. S.; Livingston, A. *J Membr Sci* 2002, 201, 65–75.
175. Scarpello, J. T.; Nair, D.; dos Santos, L. M. F.; White, L. S.; Livingston, A. *J Membr Sci* 2002, 203, 71–85.
176. Witte, P. T.; Chowdhury, S. R.; ten Elshof, J. E.; Sloboda-Rozner, D.; Neumann, R.; Alsters, P. L. *Chem Commun* 2005, 9, 1206–1208.
177. Aerts, S.; Buekenhoudt, A.; Weyten, H.; Gevers, L. E. M.; Vankelecom, I. F. G.; Jacobs, P. A. *J Membr Sci* 2006, 280, 245–252.
178. Schoeps, D.; Sashuk, V.; Ebert, K.; Plenio, H. *Organometallics* 2009, 28, 3922–3927.
179. Keraani, A.; Renouard, T.; Fischmeister, C.; Bruneau, C.; Rabiller-Baudry, M. *Chem Sus Chem* 2008, 1, 927–933.
180. Priske, M.; Wiese, K. D.; Drews, A.; Kraume, M.; Baumgarten, G. *J Membr Sci* 2010, 360, 77–83.
181. Tsoukala, A.; Peeva, L.; Livingston, A.; Bjorsvik, H. R. *Chem Sus Chem* 2012, 5, 188–193.
182. van der Gryp, P.; Barnard, A.; Cronje, J. P.; de Vlieger, D.; Marx, S.; Vosloo, H. C. M. *J Membr Sci* 2010, 353, 70–77.
183. Cano-Odena, A.; Vandecasteele, P.; Fournier, D.; Van Camp, W.; Du Prez, F. E.; Vankelecom, I. F. J. *Chem Eur J* 2010, 16, 1061–1067.
184. Han, S.; Wong, H. T.; Livingston, A. *Chem Eng Res Des* 2005, 83, 309–316.
185. Abels, C.; Redepenning, C.; Moll, A.; Melin, T.; Wessling, M. *J Membr Sci* 2012, 405, 1–10.
186. Hazarika, S.; Dutta, N. N.; Rao, P. G. *Sep Purif Technol* 2012, 97, 123–129.
187. White, L. S. *J Membr Sci* 2006, 286, 26–35.

REVIEW ARTICLE

188. Tarleton, E. S.; Robinson, J. P.; Low, J. S. *Chem Eng Res Des* 2009, 87, 271–279.
189. Othman, R.; Mohammad, A. W.; Ismail, M.; Salimon, J. *J Membr Sci* 2010, 348, 287–297.
190. Rundel, J. T.; Paul, B. K.; Reracho, V. T. *J Chromatogr A* 2007, 1162, 167–174.
191. Valadez-Blanco, R.; Ferreira, F. C.; Jorge, R. F.; Livingston, A. *J Membr Sci* 2008, 317, 50–64.
192. Sereewatthanawut, I.; Baptista, I. I.; Boam, A. T.; Hodgson, A.; Livingston, A. *J Food Eng* 2011, 102, 16–24.
193. Koncsag, C. I.; Kirwan, K. *Sep Purif Technol* 2012, 94, 54–60.
194. Darvishmanesh, S.; Robberecht, T.; Luis, P.; Degreve, J.; Van derBruggen, B. *J Am Oil Chem Soc* 2011, 88, 1255–1261.
195. Darvishmanesh, S.; Robberecht, T.; Luis, P.; Degreve, J.; Van derBruggen, B. *J Am Oil Chem Soc* 2012, 89, 959–960.
196. Kajetanowicz, A.; Czaban, J.; Krishnan, G. R.; Malinska, M.; Wozniak, K.; Siddique, H.; Peeva, L. G.; Livingston, A.; Grela, K. *Chem Sus Chem* 2013, 6, 182–912.
197. Razak, N. S. A.; Shaharun, M. S.; Mukhtarhtar, H.; Taha, M. F. *Sains Malaysiana* 2013, 42, 515–520.
198. Marchetti, P.; Butte, A.; Livingston, A. *J Membr Sci* 2012, 415, 444–458.
199. Ormerod, D.; Sledsens, B.; Vercammen, G.; Van Gool, D.; Linsen, T. *Sep Purif Technol* 2013, 115, 158–162.
200. Abejon, R.; Garea, A.; Irabien, A. *AIChE J* 2014, 60, 937–948.
201. Siddique, H.; Rundquist, E.; Bhole, Y.; Peeva, L. G.; Livingston, A. G. *J Membr Sci* 2014, 452, 354–366.
202. Sorribas, S.; Gorgojo, P.; Té llez, C.; Coronas, J.; Livingston, A. G. *J Am Chem Soc* 2013, 135, 15201–15208.
203. Shao, L.; Cheng, X. Q.; Wang, Z. X.; Ma, J.; Wang, K. Y.; Guo, Z. H. *J Membr Sci* 2014, 452, 82–89.
204. Stružynska-Piron, I.; Loccufier, J.; Vanmaele, L.; Vankelecom, I. F. *J. Chem Commun* 2013, 49, 11494–11496.
205. Firman, L. R.; Ochoa, N. A.; Marchese, J.; Pagliero, C. L. *J Membr Sci* 2013, 431, 187–196.
206. Cano-Odena, A.; Vandezande, P.; Hendrix, K.; Zaman, R.; Mostafa, K.; Egger, W.; Sperr, P.; De Baerdemaeker, J.; Vankelecom, I. F. *J Phys Chem B* 2009, 113, 10170–10176.
207. Campbell, J.; Szekely, G.; Davies, R. P.; Braddock, D. C.; Livingston, A. G. *J Mater Chem A* 2014, 2, 9260–9271.
208. Gorgojo, P.; Karan, S.; Wong, H. C.; Solomon, M. F. J.; Cabral, J. T.; Livingston, A. G. *Adv Funct Mater* (DOI: 10.1002/adfm.201400400).